Identification of a Potent and Selective Free Fatty Acid Receptor 1 (FFA1/GPR40) Agonist with Favorable Physicochemical and in Vitro ADME Properties

Elisabeth Christiansen,[†] Christian Urban,[‡] Manuel Grundmann,[§] Maria E. Due-Hansen,[†] Ellen Hagesaether,[†] Johannes Schmidt,[§] Leonardo Pardo,[∥] Susanne Ullrich,[⊥] Evi Kostenis,[§] Matthias Kassack,[‡] and Trond Ulven*,[†]

[†]Department of Physics and Chemistry, University of Southern Denmark, Campusvej 55, DK-5230 Odense M, Denmark

[‡]Institute of Pharmaceutical and Medicinal Chemistry, University of Düsseldorf, Universitätsstrasse 1, D-40225 Düsseldorf, Germany

[§]Institute for Pharmaceutical Biology, University of Bonn, Nussallee 6, D-53115 Bonn, Germany

[∥]Laboratori de Medicina Computacional, Unitat de Bioestadística, Facultat de Medicina, Universitat Autònoma de Barcelona, E-08193 Bellaterra, Barcelona, Spain

[⊥]Department of Internal Medicine, Division of Endocrinology, Diabetology and Clinical Chemistry, University of Tübingen, Otfried-Müller-Strasse 10, D-72076 Tübingen, Germany

Ⓢ Supporting Information

ABSTRACT: The free fatty acid receptor 1 (FFA1, also known as GPR40) enhances glucose-stimulated insulin secretion from pancreatic β-cells and is recognized as an interesting new target for treatment of type 2 diabetes. Several series of selective FFA1 agonists are already known. Most of these are derived from free fatty acids (FFAs) or glitazones and are relatively lipophilic. Aiming for the development of potent, selective, and less lipophilic FFA1 agonists, the terminal phenyl of a known compound series was replaced by nitrogen containing heterocycles. This resulted in the identification of **37**, a selective FFA1 agonist with potent activity on recombinant human FFA1 receptors and on the rat insulinoma cell line INS-1E, optimal lipophilicity, and excellent in vitro permeability and metabolic stability.

EC$_{50}$(FFA1) 41 nM
log D$_{7.4}$ 1.97
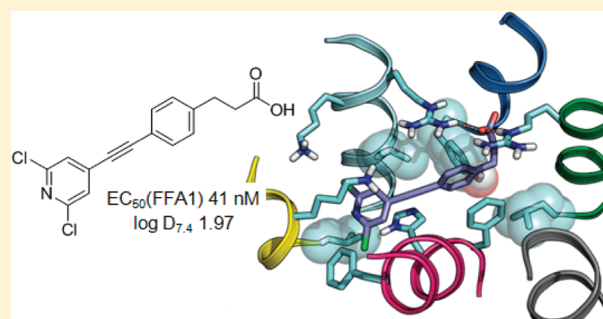
INTRODUCTION

The free fatty acid receptor 1 (FFA1/GPR40)[1] is highly expressed in pancreatic β-cells and is activated by long-chain free fatty acids (FFAs), resulting in enhancement of glucose-stimulated insulin secretion (GSIS).[2−4] It is well established that FFAs enhance GSIS but also that prolonged exposure to FFAs results in toxic effects on the β-cells. While an early study with FFA1 knockout mice suggested that FFA1 also mediates the lipotoxic effect of FFAs,[5] several other studies involving knockout mice or specific agonists have concluded that the enhancing effect on GSIS but not the lipotoxic effect is mediated by FFA1.[6−12] For example, Tan and co-workers observed that a selective FFA1 agonist improved glucose tolerance in diet-induced obese mice and that this effect was maintained after 10 days of chronic treatment.[11] Moreover, the observations that the receptor is coexpressed with various peptide hormones including the incretins GLP-1 and GIP in endocrine cells of the gastrointestinal tract and that FFA1 deficient mice exhibit reduced GLP-1 and GIP secretion suggest that FFA1 may also be involved in FFA-mediated incretin secretion and therefore may potentially enhance GSIS through a second mechanism.[13] FFA1 has attracted much interest as an antidiabetic target with the potential of increasing insulin secretion only when needed, and several series of selective agonists and antagonists have already been published (Chart 1).[11,14−22] TAK-875 and AMG-837 are both in clinical trials for treatment of type 2 diabetes.[21,23]

Lipophilicity and molecular size are factors that typically increase during the ligand optimization process and that are found to negatively influence pharmacokinetic properties and to correlate with attrition.[24−26] The concept of ligand efficiency (LE), calculated as the estimated binding energy per non-hydrogen atom, has recently become a popular measure to avoid undue increase in molecular size in the optimization process.[27] Lipophilicity, nominated as the most important druglike physical property, is found to correlate with poor oral absorption, high

Chart 1. Structures, Activities, and ClogP of Leading FFA1 Modulators[a]
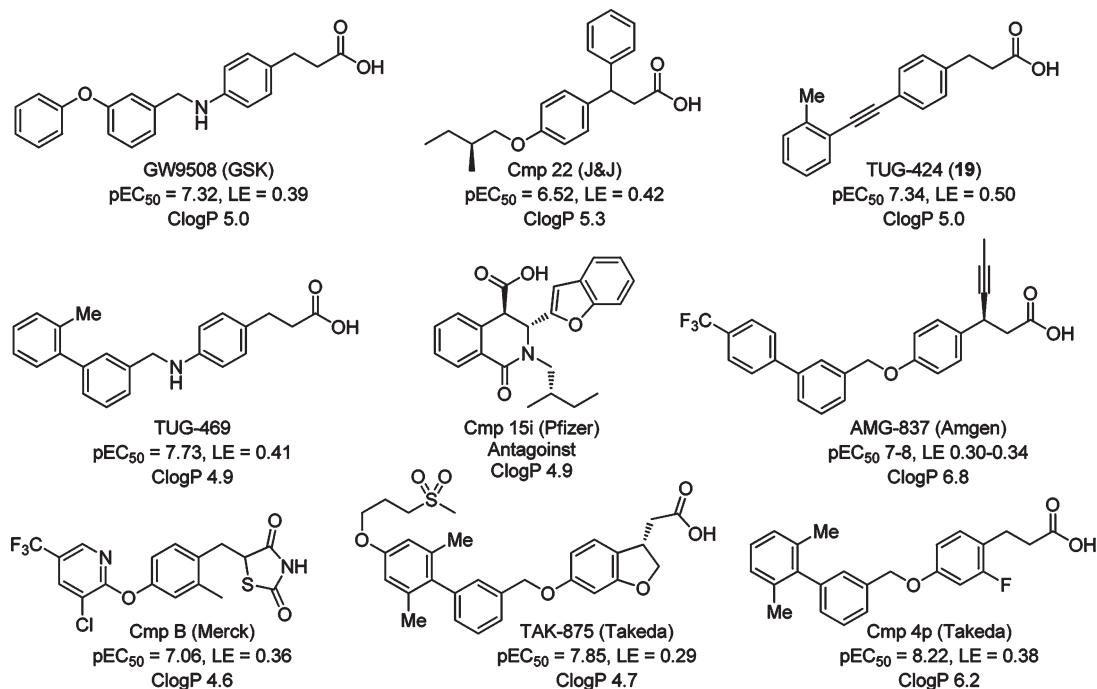

[a]ClogP values are calculated with ChemBioDraw 12.0 using the "ClogP" option.

promiscuity, high metabolic rate, toxicity, and attrition in clinical phases.[28] On the other hand, a too high hydrophilicity can result in poor permeability and rapid renal clearance. A meta-analysis of several studies on the correlation between lipophilicity and ADME properties, toxicity, promiscuity, and attrition concludes that the optimal lipophilicity when all factors are taken into account lies within the narrow log $D_{7.4}$ range between 1 and 3.[29] The nature of the FFAs indicates that the orthosteric binding site of FFA1 would be lipophilic, and compounds published hitherto, often derived from FFAs or glitazones, are indeed on the lipophilic side (Chart 1). We therefore aimed to develop potent FFA1 agonists with lower lipophilicity. Replacing a phenyl by pyridyl or a similar heterocycle generally results in significant reduction of lipophilicity. Thus, rather than extending the structure with polar substituents, we decided to investigate the effect of replacing the terminal phenyl of our recently published 4-alkynyldihydrocinnamic acid series of FFA1 agonists by more hydrophilic nitrogen-containing heterocycles.[17]

■ RESULTS AND DISCUSSION

The compounds were synthesized from the previously described central alkyne intermediate 1[30] by Sonogashira coupling with pyridyl halides (Scheme 1). We initially used a classical Sonogashira protocol (method A), but 1 proved to be a challenging substrate and we observed varying results and frequently failed reactions. A protocol reported by Beller and co-workers (method B)[31] provided the desired product in many cases where the original protocol failed but still had limitations, in particular with aryl iodides. We developed this method further, using water together with TMEDA as reaction medium, which solved the problem for the iodo substrates and turned out as a highly efficient and reliable protocol for Sonogashira coupling with pyridyl bromides and iodides (Scheme 1, method C).[30] The protocol
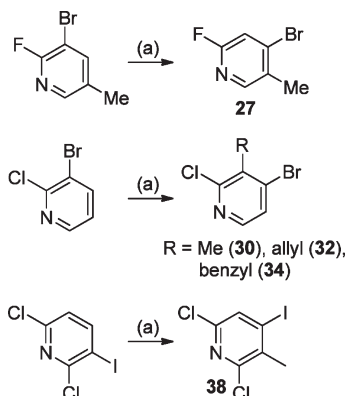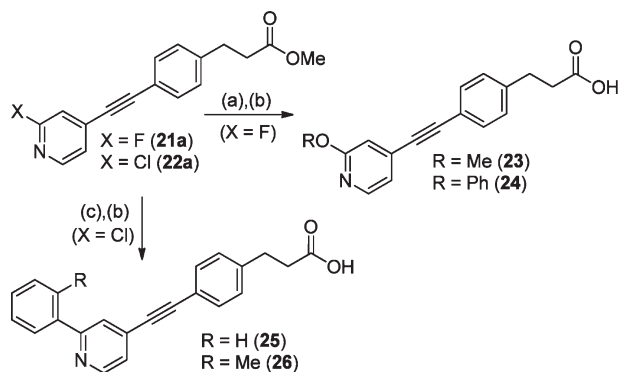
Scheme 1[a]
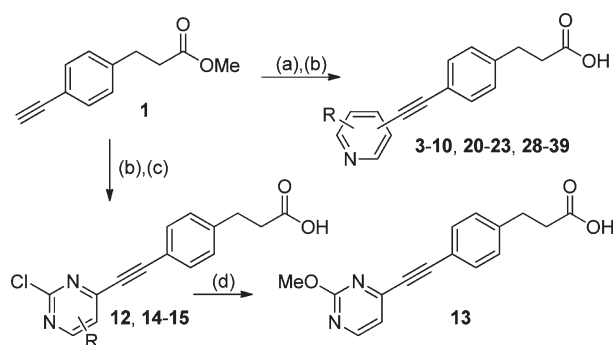
[a] Reagents and conditions: (a) pyridyl halide, method A (Pd(PPh₃)₂Cl₂, CuI, Et₃N, DMF, 50 °C), method B (Na₂PdCl₄, PIntB, CuI, TMEDA, 80 °C), or method C (Na₂PdCl₄, PIntB, CuI, TMEDA, H₂O, 80 °C); (b) LiOH, THF, H₂O, room temp; (c) 2,4-dichloropyrimidine, Pd-(PPh₃)₂Cl₂, PPh₃, CuI, THF, Et₃N, reflux; (d) NaOMe, MeOH, room temp.

however failed in the coupling with pyrimidyl chlorides. In these cases, a protocol by Deng and co-workers worked satisfactorily, although yields were low.[32]

As only a few of the desired halopyridines were commercially available, additional required halopyridines (27, 30, 32, 34, 38) were synthesized using LDA promoted halogen migration, also referred to as the "halogen dance", followed by quenching with water or electrophiles (Scheme 2).[33,34] The 2-fluoropyridyl intermediate 21a was converted to the corresponding methoxy and phenoxy analogues by nucleophilic aromatic fluoride substitution (Scheme 3), and the 2-chloropyrimidine alkyne 12 was likewise converted to the corresponding 2-methoxy analogue 13 (Scheme 1).[34] The 2-chloropyridine methyl ester 22a was converted further to

Scheme 2[a]

[a] Reagents and conditions: (a) LDA, electrophile (H₂O/MeI/allyl bromide/BnBr), THF, −78 °C.

Scheme 3[a]

[a] Reagents and conditions: (a) NaOMe, MeOH, reflux or PhOH, K₂CO₃, DMSO, 100 °C; (b) LiOH, THF, H₂O, room temp; (c) arylboronic acid, Pd(OAc)₂, SPhos, K₃PO₄, PhMe, 100 °C.

biphenyl analogues by Suzuki cross-couplings (Scheme 3). The racemic cyclopropyl carboxylic acid 43 was synthesized as outlined in Scheme 4.

Compounds were tested in a functional calcium mobilization assay on 1321N1 cells stably transfected with the human FFA1 receptor. Replacing the terminal phenyl of parent compound 2 by 2-pyridyl (3) resulted in a significant drop of activity (Table 1). A terminal 3-pyridyl (4) gave a less pronounced drop in activity, whereas the 4-pyridyl (5) was best tolerated. Some activity could be regained for the 2-pyridyl analogue by introducing a meta-methyl substituent (relative to the alkyne attachment) on the pyridine ring (6). Similarly, chloro (8 and 9) or methyl and fluoro (10) substituents on the 3-pyridyl brought the activity back to around pEC_{50} = 6.2. Ligand efficiencies were closely monitored in the optimization process, and calculated $\log P$ values (ClogP) were used as a convenient guide of lipophilicity, despite the fact that such values often are inaccurate.[35] As expected, an estimated decrease in lipophilicity on the order of 1 $\log P$ unit was observed upon substitution of the terminal phenyl by pyridyl (Table 1).

A terminal pyrimidine ring further decreased the lipophilicity of the compounds. However, none of the analogues explored (12−15) exhibited the desired potency, probably because of the

Scheme 4[a]
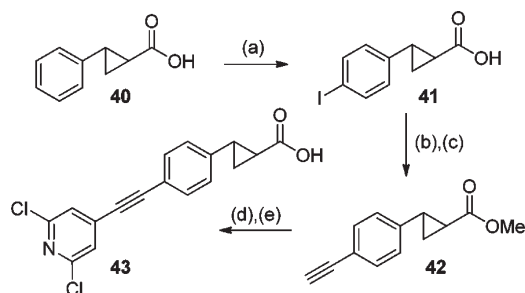
[a] Reagents and conditions: (a) KIO₃, I₂, H₂SO₄, H₂O, AcOH, reflux; (b) MeOH, HCl (cat.), room temp; (c) trimethylsilylacetylene, Na₂PdCl₄, PIntB, CuI, TMEDA, H₂O, 80 °C, then K₂CO₃, MeOH, room temp; (e) 2,6-dichloro-4-iodopyridine, Na₂PdCl₄, PIntB, CuI, TMEDA, 80 °C; (e) LiOH, H₂O, THF, room temp.

presence of the ortho-nitrogen also found to be unfavorable in 3. The direction of the nitrogen electron lone-pairs on the terminal ring appears to have significant influence on activity. The 5-thiazolyl analogue (16), with a lone-pair vector intermediate of 4 and 5, exhibited an activity similar to that of 4-pyridyl 5. To investigate the effect of the sulfur atom of 16, the corresponding 2-thienyl analogue 17 and the 3-methyl-2-thienyl 18, corresponding to the previously reported TUG-424 (19),[17] were synthesized. The compounds exhibited activities similar to those of 2 and 19, respectively, but did not result in improved activity. As sterically unhindered pyridines are known to frequently interact with CYP enzymes, we directed the focus toward compounds with 2-substituted pyridines. Methyl (20), fluoro (21), chloro (22), and methoxy (23) substituted analogues of 5 were explored, of which 22 stood out as the more potent.
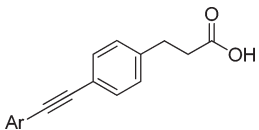
Assuming that the central alkyne of this compound series corresponds to the methyleneamino linkers found in GW9508[14,15] and TUG-469 (Chart 1),[22] the m-phenoxypyridyl 24, the biphenyl 25, and the 2′-methylbiphenyl 26 were synthesized and tested. The increased size was, however, not accompanied by increased activity, resulting in pronounced lower LE values. The lower activity of 26 compared with 25 demonstrates that the structure−activity relationships of the methyleneamino compounds cannot be transferred directly to the present series.

The 2-fluoro (21) and 2-chloro (22) analogues appeared as the most promising for further optimization. The o-methyl analogues 28, 29, and 31 showed increased potency, paralleling the SARs of 2 and 19. The larger 3-allyl 33 and 3-benzyl 35 resulted in reduced activity relative to 31, whereas chloroquinoline 36 exhibited increased activity.

The 2,6-dichloropyridine 37 provided a significant leap in activity up to pEC_{50} = 7.39, making the compound equipotent with 19. Introducing an o-methyl substituent (39) did not result in further improvement. Conformational constraint of the propionate chain by a cyclopropyl has been reported to improve the activity of the GW9508 series;[15] however, a similar constraint in 43 did not improve the activity relative to 37.

The preferred compound 37 exhibited >100-fold selectivity over the related receptors FFA2 and FFA3, which was expected despite their high homology with FFA1 because the receptors are activated by short-chain FFAs and other small carboxylic acids but not by FFAs with more than six carbon atoms or larger carboxylic acids.[36] The compound furthermore exhibited >100-fold selectivity over the nuclear receptor PPARγ and 55 other diverse receptors, ion channels, and transporters. Compounds 37

Table 1. Agonist Activities of Alkynedihydrocinnamic Acids with Heterocyclic Western Parts on FFA1

Compd	Ar	FFA1, calcium pEC50 (efficacy, %)[a]	LE[b] -Δg	ClogP[c]	Compd	Ar	FFA1, calcium pEC50 (efficacy, %)[a]	LE[b] -Δg	ClogP[c]
2[d]		6.70 ± 0.02 (108)	0.48	4.5	21		6.29 ± 0.18 (98)	0.43	3.3
3		4.88 ± 0.04 (98)	0.35	3.0	22		6.53 ± 0.03 (94)	0.45	3.8
4		5.22 ± 0.03 (96)	0.38	3.0	23		6.28 ± 0.04 (98)	0.41	3.9
5		5.39 ± 0.07 (100)	0.39	3.0	24		6.32 ± 0.04 (94)	0.33	5.1
6		5.21 ± 0.04 (108)	0.36	3.5	25		6.73 ± 0.03 (97)	0.37	5.1
7		4.96 ± 0.04 (87)	0.31	3.0	26		5.97 ± 0.04 (92)	0.31	5.3
8		6.22 ± 0.04 (91)	0.43	3.8	28		6.75 ± 0.05 (99)	0.44	3.8
9		6.15 ± 0.02 (98)	0.42	3.8	29		6.92 ± 0.04 (101)	0.45	3.8
10		6.18 ± 0.03 (98)	0.40	3.8	31		6.87 ± 0.05 (101)	0.45	4.3
12		5.04 ± 0.03 (131)	0.35	2.8	33		6.50 ± 0.04 (97)	0.39	4.9
13		5.02 ± 0.02 (109)	0.33	3.0	35		6.10 ± 0.05 (101)	0.31	5.9
14		5.37 ± 0.03 (121)	0.35	3.3	36		7.10 ± 0.07 (125)	0.41	5.2
15		5.56 ± 0.04 (110)	0.36	3.3	37		7.39 ± 0.03 (103)	0.48	4.6 (1.97[e])
16		5.41 ± 0.03 (99)	0.41	2.9	39		7.36 ± 0.04 (91)	0.46	5.1
17		6.60 ± 0.05 (97)	0.50	4.2	43	(Scheme 4)	7.37 ± 0.03 (96)	0.46	4.6
18		7.12 ± 0.04 (100)	0.51	4.7					
19[d]		7.34 ± 0.07 (102)	0.50	5.0 (2.34[e])					
20		5.95 ± 0.03 (102)	0.41	3.5					

[a] Efficacy is given as % maximal response relative to 10 μM 3-(4-benzyloxyphenyl)propionic acid (TUG-20).[22] All values were obtained in the same laboratory under identical conditions. [b] Ligand efficiencies (LE) were calculated by $-\Delta G = RT \ln K_D$, presuming that $EC_{50} \approx K_D$. Values are given in kcal mol^{-1} per non-hydrogen atom.[27] [c] Calculated by ChemBioDraw Ultra 12.0 with the "ClogP" option. [d] Previously reported (pEC$_{50}$ = 7.49 ± 0.05, obtained in a different laboratory).[17] [e] Experimentally determined log D (n-octanol/water, pH 7.4).

and the previously published **19** were also evaluated in a panel of in vitro ADME assays. Whereas **19** only exhibited moderate stability toward human liver microsomes, **37** displayed excellent properties in all assays (Table 2). Notably, **37** has good aqueous solubility and moderate lipophilicity with a log $D_{7.4}$ in the middle

of the ideal range. The compound also demonstrated high chemical stability, no inhibition of selected CYP enzymes or P-glycoprotein, and excellent Caco-2 permeability.

The permeability of **37** was, moreover, evaluated using the mucus-secreting cell-line HT29-MTX,[37] more closely mimicking

the intestinal epithelium. The compound was found to have equal or higher permeablility than ketoprofen, which is known to be rapidly and completely absorbed (37, $P_{app} = (1.64 \pm 0.08) \times 10^{-5}$ cm/s,

Table 2. Physicochemical and in Vitro ADME Properties of 19 and 37

assay	19	37
aqueous solubility (PBS, pH 7.4)	174 μM	199 μM
log D (n-octanol/PBS, pH 7.4)	2.34	1.97
chemical stability (PBS, 37 °C, 12 days)	99.9%	99.9%
plasma protein binding (human)	97.7%	96.9%
metabolic stability (human liver S9)	26%	97%
CYP inhibition (10 μM)		
CYP1A2	−8%	−7%
CYP2C9	−25%	−4%
CYP1C19	−1%	−7%
CYP2D6	0%	5%
CYP3A4	−4%	5%
P-gp inhibition (100 μM)	6.6%	−1.9%
Caco-2 (A to B, TC7, pH 6.5/7.4)	87 $\times$ 10^{-6} cm/s	112 $\times$ 10^{-6} cm/s

63% recovered; ketoprofen, $P_{app} = (1.51 \pm 0.05) \times 10^{-5}$ cm/s, 80% recovered).

The activity of 37 on FFA1 transfected HEK-293 cells was investigated in a dynamic mass redistribution (DMR) assay, enabling label-free real-time monitoring of cell activity.[38] The compound produced robust and potent activity in FFA1 transfected HEK cells, and the resulting concentration effect curve was superimposable with that obtained with the inositol monophosphate (IP_1) accumulation assay (Figure 1). The DMR assay was furthermore used to evaluate the activity of 37 on insulin secreting INS-1E cells. The compound again produced a potent and robust response in the cells. The activity could be blocked with the FFA1-selective antagonist 44 (see Supporting Information),[20] demonstrating that it is mediated through FFA1. The response translates to enhanced insulin secretion by 60% at high glucose level but does not, as expected, significantly affect insulin secretion at low glucose level (Figure 2).

The complex of 37 with human FFA1 was modeled using the crystal structure of the β_2-adrenergic receptor (β_2AR, PDB code 2RH1)[39] as template (see Experimental Section). However, hFFA1 contains the Ser-x-Pro60[II:18/2.58] motif in TM2, homologous to the Thr-x-Pro92[II:18/2.58] motif of the crystal structure of chemokine CXCR4 (PDB code 3OE0)[40] that induces a tight
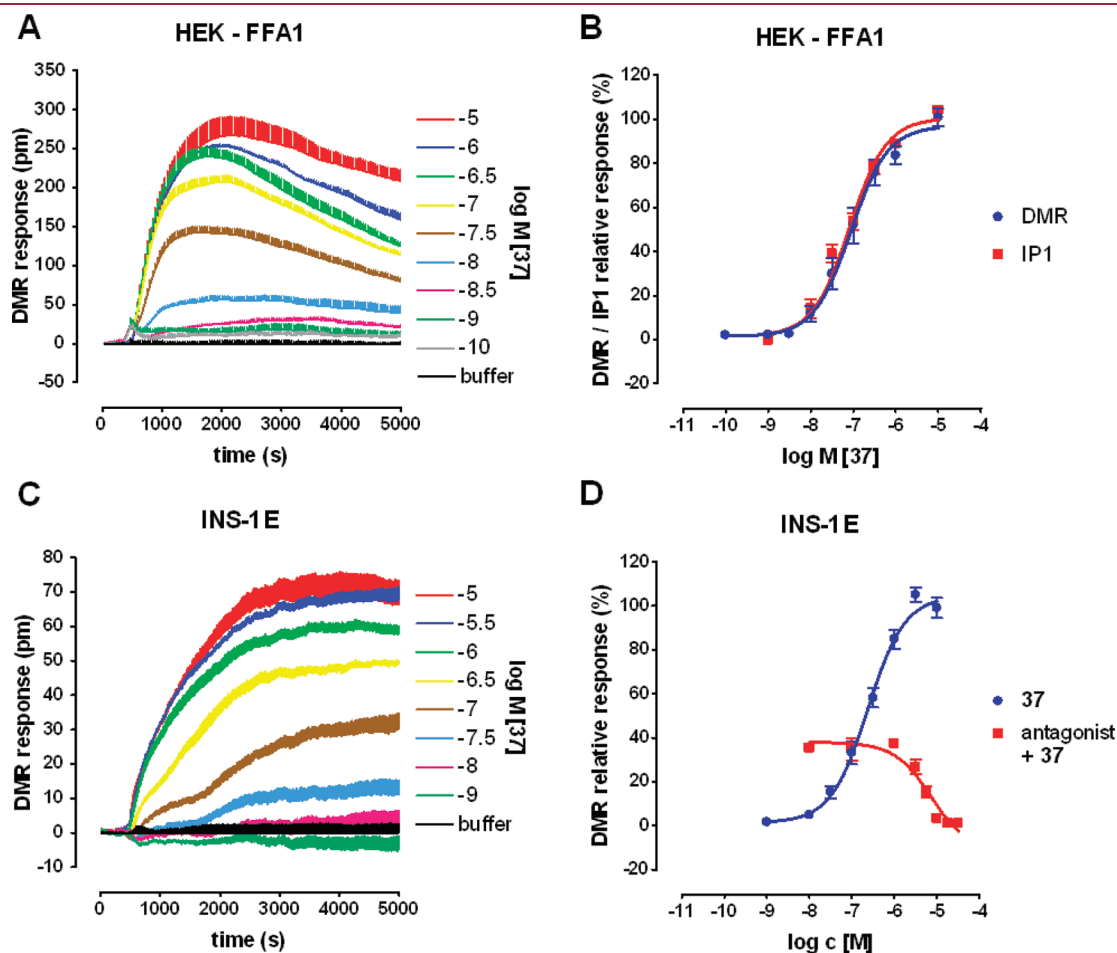

Figure 1. Activity of 37 on FFA1 transfected HEK-293 cells and on the rat β-cell line INS-1E that endogenously express FFA1. (A) Representative traces from the dynamic mass redistribution (DMR) assay of 37 on HEK-FFA1 cells. (B) Dose response curves of 37 on FFA1-HEK cells from the DMR assay (pEC$_{50}$ = 7.06 $\pm$ 0.08, n = 3) and an inositol phosphate assay (pEC$_{50}$ = 7.05 $\pm$ 0.06, n = 5). (C) Traces from the DMR assay of 37 on INS-1E cells. (D) Dose response curve of 37 on INS-1E cells (pEC$_{50}$ = 6.63 $\pm$ 0.07, n = 4) and inhibition of 37 (0.3 μM) by the FFA1 antagonist *trans*-1-oxo-3-(4-phenoxyphenyl)-2-propyl-1,2,3,4-tetrahydroisoquinoline-4-carboxylic acid (44, pIC$_{50}$ = 5.10 $\pm$ 0.07, n = 4).

helical turn of TM2. Thus, TM2 of hFFA1 was modeled in the conformation observed in CXCR4, resulting in ∼120° rotation of its extracellular end compared with other 7TM receptor structures. This rotation positions Lys62[II:20/2.60] toward the TM bundle. The model depicted in Figure 3 shows the carboxylic acid of **37** anchored between Arg183[V:05/5.39] and Arg258[VII:02/7.35], and the rigid body of the ligand was extended toward TM2 in close contact with all helices except TM1 and TM4. The central benzene ring forms aromatic—aromatic interactions with Phe87[III:09/3.33], and a twist of almost 90° between the aromatic rings places the pyridyl favorably for interaction with His86[III:08/3.32]. This mode of binding of **37** explains the observed structure—activity relationships. The *o*-methyl analogues (**19**, **28**, **29**, **31**) at the terminal aromatic ring are favored because of the presence of the hydrophobic Leu262[VII:06/7.39]. Accordingly, the presence of the polar *o*-nitrogen (2-pyridyl) in **3** is

unfavorable. In contrast, the presence of a polar binding pocket within TMs 2, 3, and 7, formed by Lys62[II:20/2.60], His86[III:02/3.32], and Lys259[VII:03/7.36], permits replacement of the terminal phenyl ring by 4-pyridyl and addition of chloro or fluoro substituents. The progressively reduced activity of **33** and **35** compared to **31** is explained by increased steric interactions of the allyl and benzyl substituents with Leu262[VII:06/7.39] and TM7, leading to displacement of the ligands toward TM3. Docking of cyclopropyl analogue **43** resulted in a conformation similar to that of the unconstrained **37** but with a slightly bent ligand, explaining that its activity is preserved but not increased. Moreover, the >100-fold selectivity of compound **37** over the highly homologous FFA2 and FFA3 receptors is attributed to the fact that these receptors replace the polar His86[III:08/3.32] by Phe and the positively charged Lys259[VII:03/7.36] by Ser or Ile, respectively (see Figure S2 in the Supporting Information).
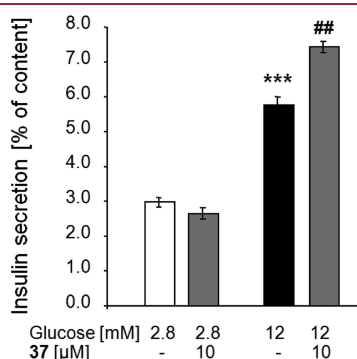
■ CONCLUSION

With the aim of developing potent FFA1 agonists with reduced lipophilicity and with our previously described alkyne ligands as starting point,[17] we have identified a new series of pyridyl FFA1 agonists. The preferred compound **37** exhibits potent full agonist activity on FFA1 and produces a potent effect in insulin secreting INS-1E cells. The compound is highly selective, is stable toward human liver microsomes, and does not inhibit any of the most important CYP enzymes. The lipophilicity of the compound is in the ideal range, and in vitro assays indicate excellent penetration. The compound therefore appears as a useful tool for in vivo exploration of FFA1 and as a lead for development of new therapeutics for treatment of type 2 diabetes.

Figure 2. Effect of **37** on glucose-stimulated insulin secretion. Mean ± SE ($n = 8$) values are shown (∗∗∗, $p < 0.005$, to 2.8 mM glucose; ##, $p < 0.05$, to 12 mM glucose).
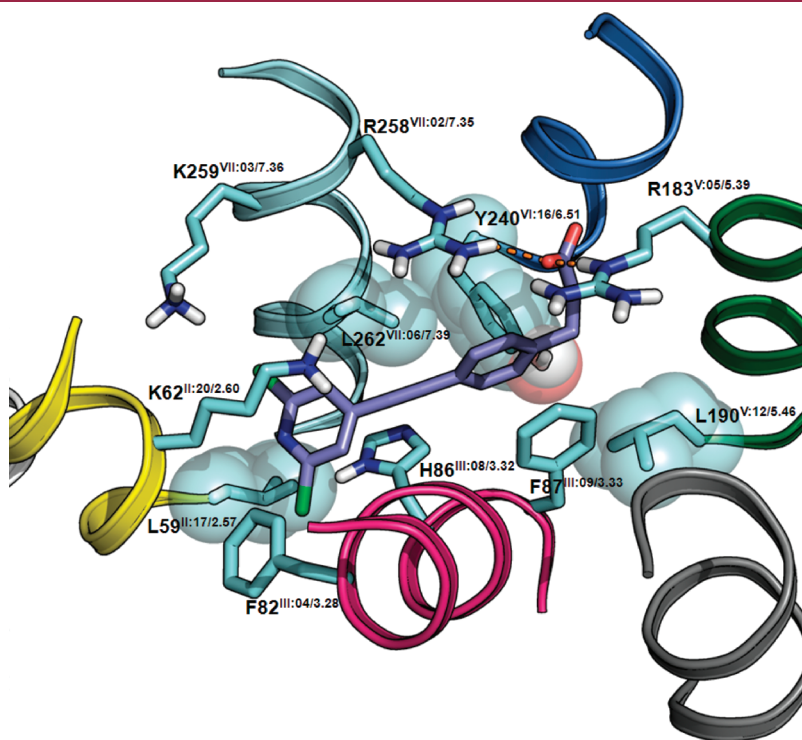

Figure 3. Model of **37** in complex with the human FFA1. Residues in direct contact with the ligand are labeled with sequence number and with Schwartz—Baldwin[41] and Ballesteros—Weinstein[42] notations given as superscript.

■ EXPERIMENTAL SECTION

All commercially available starting materials and solvents were used without further purification, unless otherwise stated. THF was freshly distilled from sodium/benzophenone. DMF, Et$_3$N, and TMEDA were dried over 4 Å sieves. Purification by flash chromatography was carried out using silica gel 60 (0.040−0.063 mm, Merck). TLC analysis was performed on silica gel 60 F$_{254}$ plates. ^{1}H and ^{13}C NMR spectra were calibrated relative to TMS internal standard or residual solvent peak. High-resolution mass spectra (HRMS) were obtained on Thermo Finnigan TSQ 700 using electrospray ionization (ESI), Bruker micrO-TOF-Q II (ESI) or IonSpec 4.7 T Ultima FTMS using DHB matrix (MALDI). Electron ionization mass spectra were obtained on a Thermo Finnigan SSQ 710 (EI). Purity was determined by HPLC and confirmed by inspection of NMR spectra. All test compounds were of ≥95% purity unless otherwise stated. HPLC analysis was performed using a Dionex 120 C18 column (5 μm, 4.6 mm × 150 mm) with 10% acetonitrile in water (0−1 min), 10−100% acetonitrile in water (1−10 min), 100% acetonitrile (11−15 min), both solvents containing 0.05% TFA as modifier, with a flow of 1 mL/min and UV detection at 230 and 254 nm.

General Procedure I-A: Sonogashira Coupling. A flame-dried Schlenk flask charged with alkyne (1 equiv), pyridyl halide (1.1 equiv), CuI (2 mol %), Et$_3$N (2.4 equiv), and DMF (2 mL/mmol) was evacuated and backfilled with inert gas three times before addition of Pd(PPh$_3$)$_2$Cl$_2$ (1 mol %) under nitrogen flow. The mixture was heated to 50 °C and stirred until consumption of the alkyne as indicated by TLC, typically overnight, then cooled to room temperature. Water was added, and the aqueous layer was extracted with EtOAc. The combined organic phases were washed with brine, dried (MgSO$_4$), and concentrated.

General Procedure I-B: Sonogashira Coupling[31]**.** A flame-dried Schlenk flask filled with argon was charged with Na$_2$PdCl$_4$ (1 mol %), 2-(di-*tert*-butylphosphino)-*N*-phenylindole (PIntB, 2 mol %), CuI (2 mol %), alkyne (1 equiv), pyridyl halide (1.1−1.5 equiv), and TMEDA (2 mL/mmol). The reaction mixture was stirred at 80 °C until consumption of the alkyne, typically overnight, then cooled to room temperature. Water was added, and the aqueous layer was extracted with EtOAc. The combined organic phases were washed with brine, dried (MgSO$_4$), and concentrated.

General Procedure I-C: Sonogashira Coupling[30]**.** A Schlenk flask filled with argon was charged with Na$_2$PdCl$_4$ (1 mol %), PIntB (2 mol %), CuI (2 mol %), alkyne (1 equiv), pyridyl halide (1.1−1.5 equiv), TMEDA (1.8 mL/mmol), and water (0.2 mL/mmol). The reaction mixture was stirred at 80 °C until consumption of the alkyne, typically 5−30 min, then cooled to room temperature. Water was added, and the aqueous layer was extracted with EtOAc. The combined organic phases were washed with brine, dried (MgSO$_4$), and concentrated.

General Procedure II: Ester Hydrolysis. The ester (1 equiv) dissolved in THF (∼5 mL/mmol) was added to LiOH·H$_2$O (2−3 equiv) in H$_2$O (∼2 mL/mmol). The mixture was stirred at room temperature until complete consumption of the starting material, as indicated by TLC, typically after 1−12 h. To the mixture was added water. The mixture was acidified with 3% HCl until pH < 1, and the aqueous layer was extracted with EtOAc. The combined extracts were washed with brine, dried (MgSO$_4$), and concentrated under vacuum.

Methyl 3-(4-(Pyridin-2-ylethynyl)phenyl)propanoate (3a). 3a was prepared from methyl 3-(4-ethynylphenyl)propanoate[30] (1, 99 mg, 0.52 mmol) and 2-iodopyridine (0.07 mL, 0.66 mmol) by general procedure I-A to give 69 mg (50%) of a pale yellow solid after purification by flash chromatography (SiO$_2$, EtOAc/petroleum ether, 1:3): R_f = 0.09 (EtOAc/petroleum ether, 1:5); ^{1}H NMR (CDCl$_3$) δ 8.62−8.60 (m, 1H), 7.70−7.64 (m, 1H), 7.54−7.49 (m, 3H), 7.25−7.18 (m, 3H), 3.67 (s, 3H), 2.97 (t, J = 7.8 Hz, 2H), 2.64 (t, J = 7.8 Hz, 2H); ^{13}C NMR (CDCl$_3$) δ 173.0, 150.0, 143.5, 141.6, 136.1, 132.2, 128.4, 127.1, 122.6, 120.2, 89.2, 88.4, 51.6, 35.2, 30.8; EI−MS m/z 265 (M$^+$).

3-(4-(Pyridin-2-ylethynyl)phenyl)propanoic Acid (3). 3 was prepared from 3a (54 mg, 0.20 mmol) by general procedure II to give 39 mg (77%) of a yellow solid: R_f 0.16 ([EtOAc with 1.25% AcOH]/petroleum ether, 1:1); ^{1}H NMR (CDCl$_3$) δ 8.64−8.63 (m, 1H), 7.74−7.68 (m, 1H), 7.63−7.49 (m, 3H), 7.29−7.21 (m, 3H), 3.00 (t, J = 7.8 Hz, 2H), 2.71 (t, J = 7.8 Hz, 2H); ^{13}C NMR (CDCl$_3$) δ 177.0, 149.4, 142.9, 141.9, 136.8, 132.2, 128.4, 127.2, 122.9, 119.9, 90.3, 87.6, 35.2, 30.6; MALDI−HRMS calcd for C$_{16}$H$_{13}$NO$_2$ (M$^+$) 252.1019, found 252.1008.

Methyl 3-(4-(Pyridin-3-ylethynyl)phenyl)propanoate (4a). 4a was prepared from 1[30] (102 mg, 0.54 mmol) and 3-iodopyridine (122 mg, 0.60 mmol) by general procedure I-A to give 27 mg (20% isolated yield, 43% based on recovered starting material) of an orange brown solid after purification by flash chromatography (SiO$_2$, EtOAc/petroleum ether, 1:3): R_f = 0.09 (EtOAc/petroleum ether, 1:5); ^{1}H NMR (CDCl$_3$) δ 8.76−7.75 (m, 1H), 7.54−7.52 (m, 1H), 7.81−7.77 (m, 1H), 7.48−7.45 (m, 2H), 7.29−7.25 (m, 1H), 7.22−7.19 (m, 2H), 3.67 (s, 3H), 2.98 (t, J = 7.8 Hz, 2H), 2.65 (t, J = 7.8 Hz, 2H); ^{13}C NMR (CDCl$_3$) δ 173.0, 152.2, 148.4, 141.5, 138.3, 131.8, 128.4, 123.0, 120.5, 120.4, 92.5, 85.7, 51.6, 35.3, 30.8; EI-MS m/z 265 (M$^+$)

3-(4-(Pyridin-3-ylethynyl)phenyl)propanoic Acid (4). 4 was prepared from 4a (24 mg, 0.09 mmol) by general procedure II to give 18 mg (79%) of an orange solid: R_f 0.16 ([EtOAc with 1.25% AcOH]/petroleum ether, 1:1); ^{1}H NMR (acetone-d_6) δ 12.60−10.70 (br s, 1H), 8.73−8.72 (m, 1H), 8.57−8.55 (m, 1H), 7.93−7.89 (m, 1H), 7.52−7.49 (m, 2H), 7.44−7.40 (m, 1H), 7.36−7.33 (m, 2H), 2.96 (t, J = 7.8 Hz, 2H), 2.65 (t, J = 7.8 Hz, 2H); ^{13}C NMR (acetone-d_6) δ 173.8, 152.6, 149.6, 143.4, 139.1, 132.5, 129.6, 124.3, 121.1, 121.0, 93.2, 86.3, 35.5, 31.4; MALDI-HRMS calcd for C$_{16}$H$_{13}$NO$_2$ (M$^+$) 252.1019, found 252.1015.

Methyl 3-(4-(Pyridin-4-ylethynyl)phenyl)propanoate (5a). 5a was prepared from 1[30] (94 mg, 0.50 mmol) and 4-bromopyridine hydrochloride (108 mg, 0.55 mmol) by general procedure I-B to give 72 mg (54%) of a white solid after purification by flash chromatography (SiO$_2$, EtOAc/petroleum ether, 1:5): R_f = 0.26 (EtOAc/petroleum ether, 1:1); ^{1}H NMR (CDCl$_3$) δ 8.52 (dd, J = 4.5, 1.5 Hz, 2H), 7.45−7.39 (m, 2H), 7.29 (dd, J = 4.5, 1.6 Hz, 2H), 7.14 (d, J = 8.3 Hz, 2H), 3.60 (s, 3H), 2.90 (t, J = 7.7 Hz, 2H), 2.57 (t, J = 7.7 Hz, 2H); ^{13}C NMR (CDCl$_3$) δ 172.0, 148.8, 141.0, 131.0, 130.5, 127.5, 124.5, 119.0, 92.9, 85.5, 50.7, 34.3, 29.8; ESI-MS m/z 288.1 (M + Na$^+$).

3-(4-(Pyridin-4-ylethynyl)phenyl)propanoic Acid (5). 5 was prepared from 5a (63 mg, 0.24 mmol) by general procedure II to give 18 mg (30%) of a white solid: R_f 0.04 (EtOAc/petroleum ether, 1:1); ^{1}H NMR (DMSO-d_6) δ 12.15 (s, 1H), 8.62 (dd, J = 4.6, 1.3 Hz, 2H), 7.58−7.46 (m, 4H), 7.33 (d, J = 8.1 Hz, 2H), 2.87 (t, J = 7.5 Hz, 2H), 2.57 (t, J = 7.6 Hz, 2H); ^{13}C NMR (DMSO-d_6) δ 173.6, 149.9, 142.9, 131.7, 130.3, 128.8, 125.3, 118.8, 93.7, 86.3, 34.7, 30.2; ESI-HRMS calcd for C$_{16}$H$_{14}$NO$_2$ (M + H$^+$) 252.1019, found 252.1016.

Methyl 3-(4-((2-Chloropyridin-3-yl)ethynyl)phenyl)propanoate (8a). 8a was prepared from 1[30] (95 mg, 0.50 mmol) and 3-bromo-2-chloropyridine (106 mg, 0.55 mmol) by general procedure I-C to give 113 mg (75%) of a pale yellow oily product after purification by flash chromatography (SiO$_2$, EtOAc/petroleum ether, 1:8): R_f = 0.24 (EtOAc/petroleum ether, 1:2); ^{1}H NMR (CDCl$_3$) δ 8.33 (dd, J = 4.8, 1.9 Hz, 1H), 7.84 (dd, J = 7.7, 1.9 Hz, 1H), 7.54−7.47 (m, 2H), 7.26−7.19 (m, 3H), 3.68 (s, 3H), 2.98 (t, J = 7.7 Hz, 2H), 2.65 (t, J = 7.7 Hz, 2H); ^{13}C NMR (CDCl$_3$) δ 173.0, 152.3, 148.1, 142.0, 141.1, 132.0, 128.5, 121.9, 120.7, 120.2, 96.8, 84.0, 51.7, 35.3, 30.9; ESI-MS m/z 322.1 (M + Na$^+$).

3-(4-((2-Chloropyridin-3-yl)ethynyl)phenyl)propanoic Acid (8). 8 was prepared from 8a (89 mg, 0.30 mmol) by general procedure II to give 79 mg (92%) of a white solid: t_R = 11.21 min (HPLC); ^{1}H NMR (DMSO-d_6) δ 12.17 (s, 1H), 8.43 (dd, J = 4.8, 1.9 Hz, 1H), 8.12 (dd, J = 7.7, 1.9 Hz, 1H), 7.56−7.46 (m, 3H), 7.34 (d, J = 8.3 Hz, 2H), 2.87

(t, J = 7.5 Hz, 2H), 2.57 (t, J = 7.6 Hz, 2H); ^{13}C NMR (DMSO-d_6) δ 173.5, 150.7, 148.9, 142.8, 141.9, 131.4, 128.8, 123.0, 119.3, 118.8, 96.4, 83.8, 34.6, 30.1; ESI-HRMS calcd for $C_{16}H_{12}ClNO_2Na$ (M + Na$^+$) 308.0449, found 308.0464.

Methyl 3-(4-((6-Chloropyridin-3-yl)ethynyl)phenyl)propanoate (9a). 9a was prepared from **1**[30] (94 mg, 0.50 mmol) and 2-chloro-5-iodopyridine (133 mg, 0.55 mmol) by general procedure I-C to give 107 mg (72%) of a white solid product after purification by flash chromatography (SiO$_2$, EtOAc/petroleum ether, 1:8): R_f = 0.35 (EtOAc/petroleum ether, 1:2); ^{1}H NMR (CDCl$_3$) δ 8.52 (dd, J = 2.3, 0.6 Hz, 1H), 7.74 (dd, J = 8.3, 2.3 Hz, 1H), 7.50−7.43 (m, 2H), 7.31 (dd, J = 8.3, 0.7 Hz, 1H), 7.24−7.18 (m, 2H), 3.67 (s, 3H), 2.98 (t, J = 7.7 Hz, 2H), 2.64 (t, J = 7.7 Hz, 2H); ^{13}C NMR (CDCl$_3$) δ 173.0, 152.0, 150.3, 141.8, 140.8, 131.9, 128.5, 123.9, 120.1, 119.5, 93.7, 84.5, 51.7, 35.3, 30.8; ESI-MS m/z 322.1 (M + Na$^+$).

3-(4-((6-Chloropyridin-3-yl)ethynyl)phenyl)propanoic Acid (9). 9 was prepared from 9a (80 mg, 0.27 mmol) by general procedure II to give 74 mg (100%) of a white solid: t_R = 11.73 min (HPLC); ^{1}H NMR (DMSO-d_6) δ 12.17 (s, 1H), 8.60 (dd, J = 2.4, 0.6 Hz, 1H), 8.03 (dd, J = 8.3, 2.4 Hz, 1H), 7.59 (dd, J = 8.3, 0.6 Hz, 1H), 7.55−7.47 (m, 2H), 7.36−7.29 (m, 2H), 2.87 (t, J = 7.5 Hz, 2H), 2.57 (t, J = 7.6 Hz, 2H); ^{13}C NMR (DMSO-d_6) δ 173.5, 151.8, 149.5, 142.6, 141.7, 131.4, 128.7, 124.3, 119.0, 118.8, 93.5, 84.4, 34.7, 30.1; ESI-HRMS calcd for $C_{16}H_{12}ClNO_2Na$ (M + Na$^+$) 308.0449, found 308.0463.

3-(4-Ethynylphenyl)propanoic Acid (11). 11 was prepared from **1**[30] (188 mg, 1.00 mmol) by general procedure II to give 165 mg (95%) of a pale yellow solid: t_R = 12.53 min (HPLC); ^{1}H NMR (CDCl$_3$) δ 11.44 (s, 1H), 7.47−7.39 (m, 2H), 7.21−7.12 (m, 2H), 3.05 (s, 1H), 2.96 (t, J = 7.7 Hz, 2H), 2.68 (t, J = 7.7 Hz, 2H); ^{13}C NMR (CDCl$_3$) δ 178.6, 141.0, 132.4, 128.3, 120.2, 83.5, 77.0, 35.2, 30.4; ESI-HRMS calcd for $C_{11}H_{10}O_2Na$ (M + Na$^+$) 197.0574, found 197.0570.

3-(4-((2-Chloropyrimidin-4-yl)ethynyl)phenyl)propanoic Acid (12). A flame-dried Schlenk flask was charged with Pd(PPh$_3$)$_2$Cl$_2$ (3 mg, 0.004 mmol, 0.5 mol %), PPh$_3$ (2 mg, 0.008 mmol, 1 mol %), THF (1 mL), Et$_3$N (1.5 mL), and 2,4-dichloropyrimidine (146 mg, 0.98 mmol) under a continuous N$_2$ flow. The solution was bubbled with N$_2$ for 15 min, and to it were added CuI (2 mg, 0.01 mmol, 1 mol %) and 11 (152 mg, 0.87 mmol). The reaction mixture was heated to reflux until consumption of the starting material, typically overnight, then cooled to room temperature. Water and aqueous HCl (1 M) were added, and the aqueous layer was extracted with EtOAc. The combined organic phases were washed with brine, dried (MgSO$_4$), and concentrated. The residue was recrystallized from AcOH/acetone (1:1) to give 71 mg (28%) of an orange solid: t_R = 10.73 min (HPLC); ^{1}H NMR (DMSO-d_6) δ 12.19 (s, 1H), 8.83 (d, J = 5.1 Hz, 1H), 7.76 (d, J = 5.1 Hz, 1H), 7.67−7.58 (m, 2H), 7.43−7.33 (m, 2H), 2.89 (t, J = 7.5 Hz, 2H), 2.58 (t, J = 7.5 Hz, 2H); ^{13}C NMR (DMSO-d_6) δ 173.5, 160.9, 160.1, 152.2, 144.2, 132.3, 129.0, 122.5, 117.3, 95.3, 85.5, 34.5, 30.2; ESI-HRMS calcd for $C_{15}H_{11}ClN_2O_2Na$ (M + Na$^+$) 309.0402, found 309.0400.

3-(4-((2-Methoxypyrimidin-4-yl)ethynyl)phenyl)propanoic Acid (13). To a dry round bottomed flask with a magnetic stirring bar and argon atmosphere were added 12 (86 mg, 0.30 mmol) and NaOMe in MeOH (0.67 mmol, 2 mL, 0.336 M). The mixture was stirred overnight. Water and aqueous HCl (1 M) were added, and the aqeuous layer was extracted with EtOAc. The organic phases were combined, washed with brine, dried (MgSO$_4$), and concentrated to give 77 mg (23%) of a white solid: t_R = 10.18 min (HPLC); ^{1}H NMR (DMSO-d_6) δ 12.19 (s, 1H), 8.66 (d, J = 4.9 Hz, 1H), 7.63−7.54 (m, 2H), 7.40−7.30 (m, 3H), 3.94 (s, 3H), 2.88 (t, J = 7.5 Hz, 2H), 2.58 (t, J = 7.5 Hz, 2H); ^{13}C NMR (DMSO-d_6) δ 173.5, 165.0, 160.3, 151.4, 143.7, 132.1, 128.9, 117.7, 117.5, 92.9, 86.5, 54.6, 34.5, 30.2; ESI-HRMS calcd for $C_{16}H_{14}N_2O_3Na$ (M + Na$^+$) 305.0897, found 305.0911.

Methyl 3-(4-((2-Methylpyridin-4-yl)ethynyl)phenyl)propanoate (20a). 20a was prepared from **1**[30] (95 mg, 0.50 mmol) and 4-iodo-2-methylpyridine (0.07 mL, 0.59 mmol) by general procedure I-B to give 62 mg (44%) of a pale yellow solid after purification by flash chromatography (SiO$_2$, EtOAc/petroleum ether, 1:5): R_f = 0.50 (EtOAc/petroleum ether, 1:2); ^{1}H NMR (CDCl$_3$) δ 8.48−8.46 (m, 1H), 7.48−7.45 (m, 2H), 7.25−7.20 (m, 4H), 3.67 (s, 3H), 2.98 (t, J = 7.8 Hz, 2H), 2.64 (t, J = 7.8 Hz, 2H), 2.56 (s, 3H); ^{13}C NMR (CDCl$_3$) δ 173.1, 158.6, 149.3, 142.0, 132.1, 131.8, 128.6, 125.1, 122.7, 120.3, 93.4, 86.9, 51.8, 35.4, 31.0, 24.5; ESI-MS m/z 302.1 (M + Na$^+$).

3-(4-((2-Methylpyridin-4-yl)ethynyl)phenyl)propanoic Acid (20). 20 was prepared from 20a (55 mg, 0.20 mmol) by general procedure II to give 58 mg (70%) of a white solid: R_f = 0.25 ([EtOAc with 1.25% AcOH]/petroleum ether, 1:1); ^{1}H NMR (DMSO-d_6) δ 8.74 (d, J = 7.6 Hz, 1H), 8.01 (s, 1H), 7.90−7.88 (m, 1H), 7.61−7.59 (m, 2H), 7.39−7.37 (m, 2H), 2.89 (t, J = 7.4 Hz, 2H), 2.73 (s, 3H), 2.58 (t, J = 7.6 Hz, 2H); ^{13}C NMR (DMSO-d_6) δ 173.4, 154.0, 144.3, 141.5, 138.3, 132.2, 129.1, 128.7, 125.5, 117.7, 100.2, 85.5, 34.6, 30.3, 19.3; ESI-HRMS calcd for $C_{17}H_{15}NO_2Na$ (M + Na$^+$) 288.0996, found 288.0989.

Methyl 3-(4-((2-Fluoropyridin-4-yl)ethynyl)phenyl)propanoate (21a). 21a was prepared from **1**[30] (352 mg, 1.87 mmol) and 4-bromo-2-fluoropyridine (210 μL, 2.04 mmol) by general procedure I-C to give 388 mg (73%) of a pale yellow solid after purification by flash chromatography (SiO$_2$, EtOAc/petroleum ether, 1:4): R_f = 0.32 (EtOAc/petroleum ether, 1:2); ^{1}H NMR (CDCl$_3$) δ 8.19 (d, J = 5.2 Hz, 1H), 7.51−7.45 (m, 2H), 7.26−7.20 (m, 3H), 7.04−6.99 (m, 1H), 3.68 (s, 3H), 2.99 (t, J = 7.7 Hz, 2H), 2.65 (t, J = 7.7 Hz, 2H); ^{13}C NMR (CDCl$_3$) δ 173.0, 163.8 (d, J = 239.4 Hz), 147.7 (d, J = 16.2 Hz), 142.4, 136.5 (d, J = 9.1 Hz), 132.2, 128.6, 123.4 (d, J = 4.0 Hz), 119.6, 111.4 (d, J = 39.4 Hz), 95.2, 85.5 (d, J = 5.1 Hz), 51.7, 35.2, 30.9; ESI-MS m/z 306.1 (M + Na$^+$).

3-(4-((2-Fluoropyridin-4-yl)ethynyl)phenyl)propanoic Acid (21). The title compound was prepared from 21a (70 mg, 0.25 mmol) by general procedure II to give 61 mg (92%) of a white solid: t_R = 11.18 min (HPLC); ^{1}H NMR (acetone-d_6) δ 10.66 (s, 1H), 8.27 (d, J = 5.1 Hz, 1H), 7.58−7.51 (m, 2H), 7.45−7.35 (m, 3H), 7.20 (s, 1H), 2.98 (t, J = 7.6 Hz, 2H), 2.66 (t, J = 7.6 Hz, 2H); ^{13}C NMR (acetone-d_6) δ 173.7, 164.8 (d, J = 236.3 Hz), 149.0 (d, J = 16.2 Hz), 144.3, 137.2 (d, J = 10.1 Hz), 132.9, 129.8, 124.4 (d, J = 4.0 Hz), 120.1, 111.9 (d, J = 40.4 Hz), 95.8, 86.0 (d, J = 6.1 Hz), 35.4, 31.4; ESI-HRMS calcd for $C_{16}H_{12}FNO_2Na$ (M + Na$^+$) 292.0745, found 292.0745.

Methyl 3-(4-((2-Chloropyridin-4-yl)ethynyl)phenyl)propanoate (22a). 22a was prepared from **1**[30] (104 mg, 0.55 mmol) and 2-chloro-4-iodopyridine (141 mg, 0.59 mmol) by general procedure I-A to give 96 mg (58%) of a pale yellow solid after purification by flash chromatography (SiO$_2$, EtOAc/petroleum ether, 1:5): R_f = 0.22 (EtOAc/petroleum ether, 1:5); ^{1}H NMR (CDCl$_3$) δ 8.36−8.35 (m, 1H), 7.48−7.45 (m, 2H), 7.42−7.41 (m, 1H), 7.29−7.26 (m, 1H), 7.24−7.21 (m, 2H), 3.67 (s, 3H), 2.99 (t, J = 7.8 Hz, 2H), 2.65 (t, J = 7.8 Hz, 2H); ^{13}C NMR (CDCl$_3$) δ 172.9, 151.7, 149.5, 142.4, 134.4, 132.1, 128.6, 125.9, 124.1, 95.4, 85.3, 51.8, 35.2, 30.8; EI-MS m/z 299 (M$^+$).

3-(4-((2-Chloropyridin-4-yl)ethynyl)phenyl)propanoic Acid (22). The title compound was prepared from 22a (73 mg, 0.24 mmol) by general procedure II to give 62 mg (90%) of a pale yellow solid: R_f = 0.09 (EtOAc/petroleum ether, 1:1); ^{1}H NMR (DMSO-d_6) δ 12.17 (s, 1H), 8.46−8.45 (m, 1H), 7.69−7.68 (m, 1H), 7.55−7.53 (m, 3H), 7.36−7.33 (m, 2H), 2.88 (t, J = 7.8 Hz, 2H), 2.58 (t, J = 7.8 Hz, 2H); ^{13}C NMR (DMSO-d_6) δ 173.5, 150.6, 150.2, 143.3, 133.6, 131.8, 128.8, 125.4, 124.6, 95.3, 85.1, 34.6, 30.2; MALDI-HRMS calcd for $C_{16}H_{12}ClNO_2$ (M$^+$) 286.0629, found 286.0626.

4-Bromo-2-fluoro-5-methylpyridine (27). To a flame-dried round-bottom flask equipped with a magnetic stirring bar filled with argon was added dry THF (5 mL). The mixture was cooled to −78 °C. LDA (1.8 M in THF/heptanes/ethylbenzene, 0.8 mL) was added, and

the mixture was stirred for 10 min before dropwise addition of the 3-bromo-2-fluoro-5-methylpyridine (274 mg, 1.44 mmol) in dry THF (1.4 mL). The mixture was stirred for 1 h before addition of water (0.5 mL, 31.3 mmol). Stirring was continued overnight. The reaction was quenched with water/THF (1:1, 1 mL), and the mixture was allowed to reach 0 °C before addition of water (2 mL) and extraction with EtOAc. The combined organic phases were washed with brine, dried (MgSO$_4$), and concentrated. Purification by flash chromatography (SiO$_2$, EtOAc/petroleum ether, 1:8) provided 257 mg (94%) of **27**: R_f = 0.37 (EtOAc/petroleum ether, 1:4); ^{1}H NMR (CDCl$_3$) δ 8.04 (s, 1H), 7.16 (d, J = 2.9 Hz, 1H), 2.35 (s, 3H); ^{13}C NMR (CDCl$_3$) δ 161.9 (d, J = 241.4 Hz), 147.4 (d, J = 15.2 Hz), 138.0 (d, J = 9.1 Hz), 131.6 (d, J = 5.1 Hz), 113.0 (d, J = 40.4 Hz), 18.6.

Methyl 3-(4-((2-Fluoro-5-methylpyridin-4-yl)ethynyl)phenyl)-propanoate (28a). 28a was prepared from **1**[30] (95 mg, 0.51 mmol) and **27** (153 mg, 0.81 mmol) by general procedure I-C to give 83 mg (55%) of a pale yellow solid after purification by flash chromatography (SiO$_2$, EtOAc/petroleum ether, 1:4): R_f = 0.29 (EtOAc/petroleum ether, 1:2); ^{1}H NMR (CDCl$_3$) δ 8.06 (s, 1H), 7.52−7.45 (m, 2H), 7.26−7.21 (m, 2H), 6.98 (d, J = 2.0 Hz, 1H), 3.68 (s, 3H), 2.99 (t, J = 7.7 Hz, 2H), 2.65 (t, J = 7.7 Hz, 2H), 2.43 (s, 3H); ^{13}C NMR (CDCl$_3$) δ 173.0, 162.1 (d, J = 237.4 Hz), 147.4 (d, J = 15.2 Hz), 142.4, 136.1 (d, J = 9.1 Hz), 132.1, 131.9 (d, J = 4.0 Hz), 128.6, 119.8, 110.7 (d, J = 39.4 Hz), 98.7, 84.7 (d, J = 5.1 Hz), 51.7, 35.3, 30.9, 16.8; ESI-MS m/z 320.1 (M + Na$^+$).

3-(4-((2-Fluoro-5-methylpyridin-4-yl)ethynyl)phenyl)pro-panoic Acid (28). 28 was prepared from **28a** (67 mg, 0.23 mmol) by general procedure II to give 63 mg (98%) of a white solid: t_R = 11.66 min (HPLC); ^{1}H NMR (DMSO-d_6) δ 12.19 (s, 1H), 8.20 (s, 1H), 7.59−7.52 (m, 2H), 7.38−7.33 (m, 2H), 7.31 (d, J = 2.1 Hz, 1H), 2.87 (d, J = 7.5 Hz, 2H), 2.57 (t, J = 7.6 Hz, 2H), 2.41 (s, 3H); ^{13}C NMR (DMSO-d_6) δ 173.5, 161.5 (d, J = 234.3 Hz), 147.5 (d, J = 16.2 Hz), 143.2, 135.3 (d, J = 10.1 Hz), 132.1 (d, J = 5.1 Hz), 131.7, 128.8, 118.5, 110.3 (d, J = 39.4 Hz), 98.7, 84.3, 34.6, 30.2, 16.2; ESI-HRMS calcd for C$_{17}$H$_{14}$FNO$_2$Na (M + Na$^+$) 306.0902, found 306.0906.

Methyl 3-(4-((2-Fluoro-3-methylpyridin-4-yl)ethynyl)phenyl)-propanoate (29a). 29a was prepared from **1**[30] (95 mg, 0.50 mmol) and 2-fluoro-4-iodo-3-methylpyridine[34] (134 mg, 0.56 mmol) by general procedure I-C to give 106 mg (71%) of a pale yellow solid after purification by flash chromatography (SiO$_2$, EtOAc/petroleum ether, 1:5): R_f = 0.37 (EtOAc/petroleum ether, 1:2); ^{1}H NMR (CDCl$_3$) δ 8.00 (d, J = 5.1 Hz, 1H), 7.52−7.46 (m, 2H), 7.25−7.19 (m, 3H), 3.68 (s, 3H), 2.99 (t, J = 7.7 Hz, 2H), 2.65 (t, J = 7.7 Hz, 2H), 2.43 (s, 3H); ^{13}C NMR (CDCl$_3$) δ 173.0, 162.4 (d, J = 238.4 Hz), 144.1 (d, J = 16.2 Hz), 142.3, 135.9 (d, J = 7.1 Hz), 132.0, 128.6, 123.6 (d, J = 4.0 Hz), 121.1 (d, J = 33.3 Hz), 119.9, 98.5, 84.6 (d, J = 6.1 Hz), 51.7, 35.3, 30.9, 12.6; ESI-MS m/z 320.1 (M + Na$^+$).

3-(4-((2-Fluoro-3-methylpyridin-4-yl)ethynyl)phenyl)pro-panoic Acid (29). 29 was prepared from **29a** (81 mg, 0.27 mmol) by general procedure II to give 72 mg (93%) of a pale yellow solid: t_R = 11.63 min (HPLC); ^{1}H NMR (DMSO-d_6) δ 12.19 (s, 1H), 8.09 (d, J = 5.1 Hz, 1H), 7.59−7.53 (m, 2H), 7.43 (d, J = 5.0 Hz, 1H), 7.37−7.32 (m, 2H), 2.88 (t, J = 7.5 Hz, 2H), 2.57 (t, J = 7.6 Hz, 2H), 2.39 (s, 3H); ^{13}C NMR (DMSO-d_6) δ 173.5, 161.6 (d, J = 234.3 Hz), 144.5 (d, J = 16.2 Hz), 143.2, 134.9 (d, J = 7.1 Hz), 131.7, 128.8, 123.7 (d, J = 4.0 Hz), 120.3 (d, J = 34.3 Hz), 118.5, 98.5, 84.2 (d, J = 6.1 Hz), 34.6, 30.2, 12.3; ESI-HRMS calcd for C$_{17}$H$_{14}$FNO$_2$Na (M + Na$^+$) 306.0902, found 306.0893.

Methyl 3-(4-((2-Chloro-3-methylpyridin-4-yl)ethynyl)phenyl)-propanoate (31a). 31a was prepared from **1**[30] (94 mg, 0.50 mmol) and 4-bromo-2-chloro-3-methylpyridine[43] (**30**, 114 mg, 0.55 mmol) by general procedure I-C to give 105 mg (67%) of a pale yellow oily product after purification by flash chromatography (SiO$_2$, EtOAc/petroleum ether, 1:10): R_f = 0.28 (EtOAc/petroleum ether, 1:2); ^{1}H NMR

(CDCl$_3$) δ 8.22−8.16 (m, 1H), 7.52−7.45 (m, 2H), 7.28 (d, J = 5.0 Hz, 1H), 7.25−7.20 (m, 2H), 3.68 (s, 3H), 2.99 (t, J = 7.7 Hz, 2H), 2.65 (t, J = 7.7 Hz, 2H), 2.57 (s, 3H); ^{13}C NMR (CDCl$_3$) δ 173.0, 152.1, 146.3, 142.3, 133.9, 133.5, 132.0, 128.6, 124.7, 119.9, 98.4, 85.2, 51.7, 35.3, 30.9, 17.9; ESI-MS m/z 336.1 (M + Na$^+$).

3-(4-((2-Chloro-3-methylpyridin-4-yl)ethynyl)phenyl)pro-panoic Acid (31). 31 was prepared from **31a** (71 mg, 0.23 mmol) by general procedure II to give 58 mg (85%) of a white solid: t_R = 12.08 min (HPLC); ^{1}H NMR (DMSO-d_6) δ 12.18 (s, 1H), 8.30−8.24 (m, 1H), 7.59−7.53 (m, 2H), 7.53−7.49 (m, 1H), 7.38−7.31 (m, 2H), 2.88 (t, J = 7.5 Hz, 2H), 2.57 (t, J = 7.6 Hz, 2H), 2.52 (s, 3H); ^{13}C NMR (DMSO-d_6) δ 173.5, 151.0, 146.8, 143.2, 133.1, 132.6, 131.7, 128.8, 125.0, 118.5, 98.3, 84.7, 34.6, 30.2, 17.5; ESI-HRMS calcd for C$_{17}$H$_{14}$ClNO$_2$Na (M + Na$^+$) 322.0606, found 322.0599.

Methyl 3-(4-((7-Chloroquinolin-4-yl)ethynyl)phenyl)pro-panoate (36a). 36a was prepared from **1**[30] (54 mg, 0.29 mmol) and 7-chloro-4-iodoquinoline (93 mg, 0.32 mmol) by general procedure I-A to give 54 mg (54%) of a beige solid after purification by flash chromatography (SiO$_2$, EtOAc/petroleum ether, 1:4): R_f = 0.06 (EtOAc/petroleum ether, 1:4); ^{1}H NMR (CDCl$_3$) δ 8.88 (d, J = 4.8 Hz, 1H), 8.27 (d, J = 9.0 Hz, 1H), 8.11 (m, 1H), 7.59−7.52 (m, 4H), 7.28−7.25 (m, 2H), 3.69 (s, 3H), 3.01 (t, J = 7.8 Hz, 2H), 2.67 (t, J = 7.8 Hz, 2H); ^{13}C NMR (CDCl$_3$) δ 172.9, 150.8, 148.5, 142.4, 135.8, 132.1, 129.9, 128.8, 128.6, 128.1, 127.4, 126.1, 123.5, 119.9, 99.2, 84.4, 51.7, 35.2, 30.9; ESI-MS m/z 372.1 (M + Na$^+$).

3-(4-((7-Chloroquinolin-4-yl)ethynyl)phenyl)propanoic Acid (36). The title compound was prepared from **36a** (50 mg, 0.14 mmol) by general procedure II to give 43 mg (90%) of a beige solid: R_f = 0.12 ([EtOAc with 1.25% AcOH]/petroleum ether, 1:2); ^{1}H NMR (DMSO-d_6) δ 12.20 (s, 1H), 8.96 (d, J = 4.5 Hz, 1H), 8.37 (d, J = 8.7 Hz, 1H), 8.15−8.14 (m, 1H), 7.78−7.74 (m, 2H), 7.68 (d, J = 8.1 Hz, 2H), 7.39 (d, J = 8.1 Hz, 2H), 2.91 (t, J = 7.5 Hz, 2H), 2.60 (t, J = 7.7 Hz, 2H); ^{13}C NMR (DMSO-d_6) δ 173.6, 151.5, 147.9, 143.4, 134.8, 132.0, 128.9, 128.6, 128.3, 128.2, 127.8, 125.4, 124.0, 118.6, 99.3, 84.0, 34.7, 30.3; ESI-HRMS calcd for C$_{20}$H$_{14}$ClNO$_2$Na (M + Na$^+$) 336.0786, found 336.0785.

3-(4-((2,6-Dichloropyridin-4-yl)ethynyl)phenyl)propanoic Acid (37). The title compound was prepared from methyl 3-(4-((2,6-dichloropyridin-4-yl)ethynyl)phenyl)propanoate[30] (296 mg, 0.90 mmol) by general procedure II to give 280 mg (99%) of a white solid: R_f = 0.54 ([EtOAc with 1.25% AcOH]/petroleum ether, 1:1); ^{1}H NMR (CDCl$_3$) δ 7.50−7.45 (m, 2H), 7.34 (s, 2H), 7.27−7.22 (m, 2H), 3.00 (t, J = 7.6 Hz, 2H), 2.71 (t, J = 7.6 Hz, 2H); ^{13}C NMR (CDCl$_3$) δ 177.7, 150.7, 142.5, 136.5, 132.3, 128.7, 124.4, 119.3, 96.8, 84.5, 34.9, 30.5; ESI-HRMS calcd for C$_{16}$H$_{11}$Cl$_2$NO$_2$Na (M + Na$^+$) 342.0060, found 342.0067.

***trans*-2-(4-Iodophenyl)cyclopropanecarboxylate (41).** To a solution of concentrated H$_2$SO$_4$ (0.1 mL) in water (1 mL) and AcOH (4 mL) were added 2-phenylcyclopropanecarboxylic acid (**40**, 200 mg, 1.23 mmol), iodine (173 mg, 0.68 mmol), and KIO$_3$ (61 mg, 0.28 mmol). The reaction mixture was heated to reflux, and to it was added AcOH (6 mL) in portions of 2 mL to rinse iodine from the condenser. After 4 h, when no further color changes appeared, the mixture was cooled to room temperature. The reaction was quenched with 1 M Na$_2$S$_2$O$_4$, and water was added. The mixture was extracted with EtOAc, and the combined extracts were washed with brine, dried (MgSO$_4$), and concentrated. The crude product was recrystallized from petroleum ether to provide 157 mg (44%) of **41** as a white solid: t_R = 11.33 min (HPLC); ^{1}H NMR (CDCl$_3$) δ 7.62−7.58 (m, 2H), 6.87−6.84 (m, 2H), 2.56−2.51 (m, 1H), 1.89−1.84 (m, 1H), 1.69−1.64 (m, 1H), 1.39−1.34 (m, 1H); ^{13}C NMR (CDCl$_3$) δ 179.3, 139.2, 137.6, 128.3, 91.7, 26.5, 23.9, 17.4; ESI-MS m/z 311.0 (M + Na$^+$).

Methyl 2-(4-Ethynylphenyl)cyclopropanecarboxylate (42). Methanol (16 mL) under argon at 0 °C was added to AcCl (1.3 mL,

18.3 mmol). The mixture was stirred for 10 min before slow addition of **41** (1.65 g, 5.74 mmol). The mixture was stirred for an additional 3 h at room temperature before the mixture was concentrated under vacuum, redissolved in MeOH, and concentrated to give 1.68 g (97%) of the methyl ester as a pure white solid: t_R = 13.24 min (HPLC).

A Schlenk flask charged with the methyl ester (2.56 g, 8.47 mmol), Na₂PdCl₄ (25 mg, 0.08 mmol), 2-(di-*tert*-butylphosphino)-1-phenylindole (PIntB, 57 mg, 0.17 mmol), CuI (32 mg, 0.17 mmol), water (1.7 mL), and TMEDA (15.3 mL) was evacuated and backfilled with argon three times and heated to 70 °C. Trimethylsilylacetylene (2.1 mL, 16.4 mmol) was added, and the temperature was elevated to 80 °C. After 30 min, consumption of the starting material was confirmed by HPLC, and the reaction mixture was cooled to room temperature. Water was added, and the aqueous layer was extracted with EtOAc. The combined extracts were washed with brine, dried (MgSO₄), concentrated, and used directly in the next step: t_R = 14.56 min (HPLC).

To methyl 3-(4-((trimethylsilyl)ethynyl)phenyl)cyclopropanecarboxylate (2.24 g, 8.47 mmol) and potassium carbonate (2.34 g, 16.95 mmol) was added MeOH (85 mL), and the mixture was stirred vigorously for 1 h at room temperature. To the mixture was added water, and the aqueous layer was extracted with EtOAc. The organic phases were combined, washed with brine, dried (MgSO₄), and concentrated. The residue was purified by flash chromatography (SiO₂, EtOAc/petroleum ether, 1:5) to give 1.59 g (97%) of **42** as a pale yellow solid: R_f = 0.60 (EtOAc/petroleum ether, 1:1); ¹H NMR (CDCl₃) δ 7.43−7.37 (m, 2H), 7.07−7.01 (m, 2H), 3.72 (s, 3H), 3.06 (s, 1H), 2.51 (ddd, J = 9.2, 6.5, 4.2 Hz, 1H), 1.91 (ddd, J = 8.5, 5.4, 4.2 Hz, 1H), 1.63 (ddd, J = 9.2, 5.3, 4.7 Hz, 1H), 1.32 (ddd, J = 8.4, 6.5, 4.7 Hz, 1H); ¹³C NMR (CDCl₃) δ 173.5, 141.0, 132.3, 126.1, 120.2, 83.4, 77.2, 52.0, 26.1, 24.2, 17.2.

Methyl 2-(4-((2,6-Dichloropyridin-4-yl)ethynyl)phenyl)-cyclopropanecarboxylate (43a). **43a** was prepared from **42** (80 mg, 0.40 mmol) and 2,6-dichloro-4-iodopyridine (121 mg, 0.44 mmol) by general procedure I-B to give 19 mg (23%) of a white solid after purification by flash chromatography (SiO₂, EtOAc/petroleum ether, 1:10): R_f = 0.36 (EtOAc/petroleum ether, 1:4); ¹H NMR (CDCl₃) δ 7.45 (d, J = 8.2 Hz, 2H), 7.34 (s, 2H), 7.11 (d, J = 8.2 Hz, 2H), 3.73 (s, 3H), 2.61−2.48 (m, 1H), 2.02−1.90 (m, 1H), 1.67 (dt, J = 10.0, 5.1 Hz, 1H), 1.35 (ddd, J = 8.4, 6.4, 4.8 Hz, 1H); ¹³C NMR (CDCl₃) δ 173.4, 150.7, 142.5, 136.5, 132.2, 126.4, 124.4, 119.2, 96.7, 84.7, 52.1, 26.1, 24.4, 17.3; ESI-MS m/z 368.1 (M + Na⁺).

2-(4-((2,6-Dichloropyridin-4-yl)ethynyl)phenyl)cyclopro-panecarboxylic Acid (43). **43** was prepared from **43a** (16 mg, 0.05 mmol) by general procedure II to give 14 mg (88%) of a white solid: R_f = 0.37 ([EtOAc with 1.25% AcOH]/petroleum ether, 1:1); ¹H NMR (acetone-d_6) δ 7.47−7.40 (m, 4H), 7.17 (d, J = 8.3 Hz, 2H), 2.43−2.33 (m, 1H), 1.84 (ddd, J = 9.3, 5.2, 4.2 Hz, 1H), 1.44 (dt, J = 9.6, 4.9 Hz, 1H), 1.35−1.29 (m, 1H); ¹³C NMR (acetone-d_6) δ 173.9, 151.2, 144.2, 137.7, 133.1, 127.4, 125.4, 119.9, 97.5, 85.3, 26.5, 25.0, 17.7; ESI-HRMS calcd for $C_{18}H_{13}Cl_2NO_2Na$ (M + Na⁺) 354.0060, found 354.0055.

Materials, Cell Culture, and Cell Lines. Tissue culture media reagents were purchased from Invitrogen, Karlsruhe, Germany, unless otherwise explicitly specified. 1321N1 cells stably transfected with human FFA1 were grown in Dulbecco's modified Eagle's medium supplemented with 10% (v/v) heat-inactivated fetal calf serum, 1% sodium pyruvate, 100 U/mL penicillin, 100 μg/mL streptomycin, and 400 μg/mL G418. Rat INS-1E cells for DMR studies were cultivated in RPMI 1640+ GlutaMAX−I medium supplemented with 10% (v/v) fetal calf serum (FCS), 100 U/mL penicillin, 100 μg/mL streptomycin, and 50 μM 2-mercaptoethanol, and INS-1E cells for insulin secretion studies were cultivated in RPMI 1640 medium supplemented with 10% (v/v) fetal calf serum (FCS), 10 mM HEPES, 2 mM glutamine, 1 mM Na pyruvate, 50 μM 2-mercaptoethanol. Flp-In T-Rex HEK293 cells (Invitrogen) stably expressing human FLAG-tagged FFA1 (FFA1-HEK) in a doxycycline-dependent manner[22] were maintained in

high-glucose Dulbecco's modified Eagle's medium (DMEM) supplemented with 10% FCS, 100 U/mL penicillin, 100 μg/mL streptomycin, 100 μg/mL hygromycin B, and 15 μg/mL blasticidin (InvivoGen, Toulouse, France). Expression of FFA1 from the Flp-In locus was induced by treatment with 1 μg/mL doxycycline (Sigma-Aldrich, Taufkirchen, Germany) for 16 h. All cells were cultivated with 5% CO₂ at 37 °C in a humidified atmosphere.

Calcium Mobilization Assays. Calcium measurements were performed using a NOVOstar microplate reader with a built-in pipetor (BMG LabTech, Offenburg, Germany). Cells were seeded in 96-well tissue-culture plates at a density of 30000−40000 cells per well. After 24 h, cells were washed twice in Krebs-HEPES buffer (KHB, 118.6 mM NaCl, 4.7 mM KCl, 1.2 mM KH₂PO₄, 4.2 mM NaHCO₃, 11.7 mM D-glucose, 10 mM HEPES (free acid), 1.3 mM CaCl₂, and 1.2 mM MgSO₄, pH 7.4) and loaded with 1.5 μM Oregon Green 488 BAPTA-1/AM (Molecular Probes, Eugene, OR) and 0.03% Pluronic F-127 (Invitrogen, Karlsruhe, Germany) for 1 h (37 °C, 5% CO₂). After addition of KHB, microplates were directly transferred to Novostar and kept at 37 °C under exclusion of light for 15 min until the measurement was started. For testing of agonists, 20 μL of a 10-fold concentrated test compound solution was injected sequentially into separate wells and fluorescence was measured at 520 nm (bandwidth 25 nm) for 50 intervals of 0.4 s each. The excitation wavelength was 485 nm (bandwidth 25 nm).

Label-Free Dynamic Mass Redistribution (DMR) Assay. A beta version of the label-free Corning Epic biosensor was used consisting of an optical detection unit, a temperature-control unit, and an integrated robotic liquid handling device. The method has been validated recently in Schröder et al.[38] Refractive waveguide grating optical biosensors, integrated in Epic 384-well microplates (Corning, NY, U.S.), allow extremely sensitive measurements of the index of refraction in a detecting zone 150 nm above the surface of the sensor. Mass movements of cellular constituents (dynamic mass redistribution, DMR) induced upon GPCR activation can be detected by illuminating the underside of the microplate with broadband light. The Epic instrument measures changes in wavelength of the outgoing light that is a sensitive function of the index of refraction. The magnitude of this wavelength shift (in picometers) is directly proportional to the amount of DMR. At 24 h before the assay INS-1E and FFA1-HEK cells were seeded onto fibronectin-coated 384-well Epic sensor microplates at a density of 30 000 (INS-1E) and 15 000 (FFA1-HEK) cells/well and cultured for 20−24 h (37 °C, 5% CO₂) to obtain confluent monolayers. After removal of medium, cells were washed twice with Hank's buffered salt solution (HBSS) containing 20 mM HEPES and kept for 1 h in the Epic reader at a constant temperature of 28 °C. Hereafter, the sensor plate was scanned and a baseline optical signature was recorded. Compound solutions were then transferred into the sensor plate, and DMR was monitored for at least 5000 s.

IP₁ Accumulation Assays. The HTRF-IP One kit (CIS Bio International, Gif-sur-Yvette Cedex, France) was used for measuring IP₁ production in cells expressing FFA1. In a 384-well format, the cell suspension was dispensed at (100 000 cells/7 μL)/well. Following 20 min of incubation at 37 °C, an amount of 7 μL of stimulation buffer (HBSS, 10 mM HEPES and 50 mM LiCl) containing various concentrations of ligands was added. After 30 min, an amount of 3 μL of IP₁-d2 conjugate followed by 3 μL of Europium cryptate-labeled anti-IP₁ antibody was added to each well. After incubation at room temperature for 60 min, time-resolved fluorescence at 620 and 665 nm was measured with the Mithras LB 940 multimode reader (Berthold Technologies, Bad Wildbad, Germany). Results were calculated from the 665 nm/620 nm ratio and expressed as ΔF (ΔF (%) = [(standard or sample ratio − ratio$_{neg}$)/ratio$_{neg}$] × 100). Data were normalized to the maximum IP₁ response obtained with 10 μM **37**.

Insulin Secretion. INS-1E cells were seeded at a density of 100 000 cells/mL in 24-well plates for 2 days and incubated as described

previously.[44] In brief, cells were incubated for 1 h at 37 °C in a solution containing 136 mM NaCl, 4.7 mM KCl, 1.2 mM KH$_2$PO$_4$, 1.2 mM MgSO$_4$, 1 mM CaCl$_2$, 5 mM NaHCO$_3$, 10 mM HEPES, 0.5 g/L bovine serum albumin (fatty acid free, Sigma, Deisenhofen, Germany), pH 7.4, and the test substance as indicated. Insulin released into the supernatant and insulin content after acid ethanol extraction were determined by radioimmunoassay (Linco, U.S.).

Permeability in Mucus-Expressing Cells[37]. The HT29-MTX cell line for permeability studies was kindly provided by Dr. Thècla Lesuffleur (INSERM UMR S 938, Paris, France). Details regarding cell medium, growth, and seeding, as well as the permeability experiments including monolayer integrity and calculations of P_{app} (cm/s), are described elsewhere.[45] Cells of passage number 32 were grown for 23 days (TEER > 750 $\Omega \cdot$cm^2) before permeability studies were conducted. The permeation of **37** and ketoprofen (the drugs were dissolved at 10 mM in dimethylsulfoxide followed by diluting 1:100 in buffer, giving a concentration of 100 μM) was tested at 15, 30, 45, and 60 min at 37 °C and 50 rpm. The drugs were quantified using HPLC analysis. Nonpermeated drug was also measured to estimate the recovery. At the end of the experiments, the integrity of the cell monolayers were monitored by testing the permeation of the paracellular marker carboxyfluorescein (20 μM) after 1 h and measuring TEER. The results for the permeation experiments are presented as the mean and standard deviation of three parallels.

Counterscreens. Counterscreening on a panel of 56 receptors, ion channels, and transporters (PPARγ, A$_1$, A$_{2A}$, A$_3$, α_1, α_2, β_1, β_2, AT$_1$, BZD (central), B$_2$, CB$_1$, CCK$_1$, D$_1$, D$_{2S}$, ETA, GABA, GAL$_2$, CXCR2, CCR1, H$_1$, H$_2$, MC$_4$, MT$_1$, M$_1$, M$_2$, M$_3$, NK$_2$, NK$_3$, Y$_1$, Y$_2$, NTS$_1$, δ_2 (DOP), κ (KOP), μ (MOP), NOP (ORL1), TP (TXA$_2$/PGH$_2$), 5-HT$_{1A}$, 5-HT$_{1B}$, 5-HT$_{2A}$, 5-HT$_{2B}$, 5-HT$_3$, 5-HT$_{5a}$, 5-HT$_6$, 5-HT$_7$, sst, VPAC$_1$ (VIP$_1$), V$_{1a}$, Ca^{2+} channel (L, verapamil site, phenylalkylamine), K$_V$ channel, SK$_{Ca}$ channel, Na$^+$ channel (site 2), Cl$^-$ channel (GABA-gated), norepinephrine transporter, dopamine transporter, and 5-HT transporter) was performed at Cerep Inc. Counterscreens on FFA2 and FFA3 were performed on HEK293 cells stably transfected to express hFFA2 and hFFA3, respectively, using the label-free DMR assay essentially as described above for FFA1-HEK cells. The test compound was dissolved in DMSO to a 10 mM stock solution, which was diluted with water or HBSS to a final test concentration of 10 μM.

Molecular Modeling. Modeller 9v8[46] was used to build a homology model of hFFA1 using both the crystal structure of chemokine CXCR4[40] (PDB code 3OE0) for TM2 and the crystal structure of the β_2-adrenergic receptor[39] (PDB code 2RH1) for the remaining receptor. The rationale for this approach is that the longer TMs 6 and 7 of CXCR4 are incompatible with hFFA1. TM1 of CXCR4 is bent toward the center of the bundle because of a disulfide bridge between the N terminus and Cys$^{7.25}$ that is absent in hFFA1, and hFFA1 contains the Ser-x-Pro60$^{II:18/2.58}$ motif in TM2, homologous to the Thr-x-Pro92$^{II:18/2.58}$ motif of CXCR4, that induces a tight helical turn of TM2 (see Figure S2 in the Supporting Information for sequence alignments). The second extracellular loop of hFFA1 was arbitrarily modeled as in the β_2AR, formed by a helical segment, instead of as in CXCR4, formed by two β-strands. The Glu145-Arg183$^{V:05/5.39}$ and Glu172-Arg258$^{VII:02/7.35}$ ionic locks previously reported by Sum et al.,[47] together with the disulfide bridge between Cys79$^{III:01/3.25}$ and Cys170, were included in the model. The ligand was minimized using Gaussian 03[48] and manually docked so that the carboxylic group interacted with Arg183$^{V:05/5.39}$ and Arg258$^{VII:02/7.35}$, as described by mutational studies[49] using PyMOL[50] as graphical interface. Afterward, the ligand—receptor complex was energy-optimized using the Sander module of AMBER 9.[51] The Duan et al. force field[52] was used for the receptor, and the general AMBER force field (GAFF) and HF/6-31G*-derived RESP atomic charges were used for the ligands.

■ ASSOCIATED CONTENT

S **Supporting Information.** Synthetic procedures and compound characterization, activity of **19** compared to **37** in IP1 and DMR assays, and receptor sequence alignments. This material is available free of charge via the Internet at http://pubs.acs.org.

■ AUTHOR INFORMATION

Corresponding Author
*Phone: +45 6550 2568. Fax: +45 6615 8780. E-mail: ulven@ifk.sdu.dk.

■ ACKNOWLEDGMENT

■ ABREVIATIONS USED

ADME, absorption, distribution, metabolism, and excretion; AR, adrenergic receptor; CYP, cytochrome P450; DHB, 2,5-dihydroxybenzoic acid; DMR, dynamic mass redistribution; ECL, extracellular loop; FFA, free fatty acid; FFA1, free fatty acid receptor 1 (GPR40); FFA2, free fatty acid receptor 2 (GPR43); FFA3, free fatty acid receptor 3 (GPR41); HBSS, Hank's balanced salt solution; HEK, human embryonic kidney; GIP, gastric inhibitory polypeptide; GLP-1, glucagon-like peptide 1; GSIS, glucose-stimulated insulin secretion; LE, ligand efficiency; PBS, phosphate buffered saline; P-gp, P-glycoprotein; PIntB, 2-(di-*tert*-butylphosphino)-1-phenylindole; PPARγ, peroxisome proliferator-activated receptor γ; SAR, structure—activity relationship; SPhos, 2-dicyclohexylphosphino-2′,6′-dimethoxybiphenyl; TM, transmembrane; TMEDA, N,N,N',N'-tetramethylethylenediamine

■ REFERENCES

(1) The name FFA1 is designated by the International Union of Basic and Clinical Pharmacology to the receptor previously called GPR40 (http://www.iuphar.org/).

(2) Itoh, Y.; Kawamata, Y.; Harada, M.; Kobayashi, M.; Fujii, R.; Fukusumi, S.; Ogi, K.; Hosoya, M.; Tanaka, Y.; Uejima, H.; Tanaka, H.; Maruyama, M.; Satoh, R.; Okubo, S.; Kizawa, H.; Komatsu, H.; Matsumura, F.; Noguchi, Y.; Shinobara, T.; Hinuma, S.; Fujisawa, Y.; Fujino, M. Free fatty acids regulate insulin secretion from pancreatic beta cells through GPR40. *Nature* **2003**, *422*, 173–176.

(3) Briscoe, C. P.; Tadayyon, M.; Andrews, J. L.; Benson, W. G.; Chambers, J. K.; Eilert, M. M.; Ellis, C.; Elshourbagy, N. A.; Goetz, A. S.; Minnick, D. T.; Murdock, P. R.; Sauls, H. R.; Shabon, U.; Spinage, L. D.; Strum, J. C.; Szekeres, P. G.; Tan, K. B.; Way, J. M.; Ignar, D. M.; Wilson, S.; Muir, A. I. The orphan G protein-coupled receptor GPR40 is activated by medium and long chain fatty acids. *J. Biol. Chem.* **2003**, *278*, 11303–11311.

(4) Kotarsky, K.; Nilsson, N. E.; Flodgren, E.; Owman, C.; Olde, B. A human cell surface receptor activated by free fatty acids and thiazolidinedione drugs. *Biochem. Biophys. Res. Commun.* **2003**, *301*, 406–410.

(5) Steneberg, R.; Rubins, N.; Bartoov-Shifman, R.; Walker, M. D.; Edlund, H. The FFA receptor GPR40 links hyperinsulinemia, hepatic

steatosis, and impaired glucose homeostasis in mouse. *Cell Metab.* **2005**, *1*, 245–258.

(6) Latour, M. G.; Alquier, T.; Oseid, E.; Tremblay, C.; Jetton, T. L.; Luo, J.; Lin, D. C. H.; Poitout, V. GPR40 is necessary but not sufficient for fatty acid stimulation of insulin secretion in vivo. *Diabetes* **2007**, *56*, 1087–1094.

(7) Kebede, M.; Alquier, T.; Latour, M. G.; Semache, M.; Tremblay, C.; Poitout, V. The fatty acid receptor GPR40 plays a role in insulin secretion in vivo after high-fat feeding. *Diabetes* **2008**, *57*, 2432–2437.

(8) Lan, H.; Hoos, L. M.; Liu, L.; Tetzloffl, G.; Hu, W. W.; Abbondanzo, S. J.; Vassileva, G.; Gustafson, E. L.; Hedrick, J. A.; Davis, H. R. Lack of FFAR1/GPR40 does not protect mice from high-fat diet-induced metabolic disease. *Diabetes* **2008**, *57*, 2999–3006.

(9) Nagasumi, K.; Esaki, R.; Iwachidow, K.; Yasuhara, Y.; Ogi, K.; Tanaka, H.; Nakata, M.; Yano, T.; Shimakawa, K.; Taketomi, S.; Takeuchi, K.; Odaka, H.; Kaisho, Y. Overexpression of GPR40 in pancreatic beta-cells augments glucose-stimulated insulin secretion and improves glucose tolerance in normal and diabetic mice. *Diabetes* **2009**, *58*, 1067–1076.

(10) Alquier, T.; Peyot, M. L.; Latour, M. G.; Kebede, M.; Sorensen, C. M.; Gesta, S.; Kahn, C. R.; Smith, R. D.; Jetton, T. L.; Metz, T. O.; Prentki, M.; Poitout, V. Deletion of GPR40 impairs glucose-induced insulin secretion in vivo in mice without affecting intracellular fuel metabolism in islets. *Diabetes* **2009**, *58*, 2607–2615.

(11) Tan, C. P.; Feng, Y.; Zhou, Y. P.; Eiermann, G. J.; Petrov, A.; Zhou, C. Y.; Lin, S. N.; Salituro, G.; Meinke, P.; Mosley, R.; Akiyama, T. E.; Einstein, M.; Kumar, S.; Berger, J. P.; Mills, S. G.; Thornberry, N. A.; Yang, L. H.; Howard, A. D. Selective small-molecule agonists of G protein-coupled receptor 40 promote glucose-dependent insulin secretion and reduce blood glucose in mice. *Diabetes* **2008**, *57*, 2211–2219.

(12) Stoddart, L. A.; Smith, N. J.; Milligan, G. International Union of Pharmacology. LXXI. Free fatty acid receptors FFA1, -2, and -3: pharmacology and pathophysiological functions. *Pharmacol. Rev.* **2008**, *60*, 405–417.

(13) Edfalk, S.; Steneberg, P.; Edlund, H. Gpr40 is expressed in enteroendocrine cells and mediates free fatty acid stimulation of incretin secretion. *Diabetes* **2008**, *57*, 2280–2287.

(14) Briscoe, C. P.; Peat, A. J.; McKeown, S. C.; Corbett, D. F.; Goetz, A. S.; Littleton, T. R.; McCoy, D. C.; Kenakin, T. P.; Andrews, J. L.; Ammala, C.; Fornwald, J. A.; Ignar, D. M.; Jenkinson, S. Pharmacological regulation of insulin secretion in MIN6 cells through the fatty acid receptor GPR40: identification of agonist and antagonist small molecules. *Br. J. Pharmacol.* **2006**, *148*, 619–628.

(15) Garrido, D. M.; Corbett, D. F.; Dwornik, K. A.; Goetz, A. S.; Littleton, T. R.; McKeown, S. C.; Mills, W. Y.; Smalley, T. L.; Briscoe, C. P.; Peat, A. J. Synthesis and activity of small molecule GPR40 agonists. *Bioorg. Med. Chem. Lett.* **2006**, *16*, 1840–1845.

(16) Song, F. B.; Lu, S. F.; Gunnet, J.; Xu, J. Z.; Wines, P.; Proost, J.; Liang, Y.; Baumann, C.; Lenhard, J.; Murray, W. V.; Demarest, K. T.; Kuo, G. H. Synthesis and biological evaluation of 3-aryl-3-(4-phenoxy)-propionic acid as a novel series of G protein-coupled receptor 40 agonists. *J. Med. Chem.* **2007**, *50*, 2807–2817.

(17) Christiansen, E.; Urban, C.; Merten, N.; Liebscher, K.; Karlsen, K. K.; Hamacher, A.; Spinrath, A.; Bond, A. D.; Drewke, C.; Ullrich, S.; Kassack, M. U.; Kostenis, E.; Ulven, T. Discovery of potent and selective agonists for the free fatty acid receptor 1 (FFA1/GPR40), a potential target for the treatment of type II diabetes. *J. Med. Chem.* **2008**, *51*, 7061–7064.

(18) Tikhonova, I. G.; Sum, C. S.; Neumann, S.; Engel, S.; Raaka, B. M.; Costanzi, S.; Gershengorn, M. C. Discovery of novel agonists and antagonists of the free fatty acid receptor 1 (FFAR1) using virtual screening. *J. Med. Chem.* **2008**, *51*, 625–633.

(19) Bharate, S. B.; Nemmani, K. V. S.; Vishwakarma, R. A. Progress in the discovery and development of small-molecule modulators of G-protein-coupled receptor 40 (GPR40/FFA1/FFAR1): an emerging target for type 2 diabetes. *Expert Opin. Ther. Pat.* **2009**, *19*, 237–264.

(20) Humphries, P. S.; Benbow, J. W.; Bonin, P. D.; Boyer, D.; Doran, S. D.; Frisbie, R. K.; Piotrowski, D. W.; Balan, G.; Bechle, B. M.; Conn, E. L.; Dirico, K. J.; Oliver, R. M.; Soeller, W. C.; Southers, J. A.; Yang, X. J. Synthesis and SAR of 1,2,3,4-tetrahydroisoquinolin-1-ones as novel G-protein-coupled receptor 40 (GPR40) antagonists. *Bioorg. Med. Chem. Lett.* **2009**, *19*, 2400–2403.

(21) Negoro, N.; Sasaki, S.; Mikami, S.; Ito, M.; Suzuki, M.; Tsujihata, Y.; Ito, R.; Harada, A.; Takeuchi, K.; Suzuki, N.; Miyazaki, J.; Santou, T.; Odani, T.; Kanzaki, N.; Funami, M.; Tanaka, T.; Kogame, A.; Matsunaga, S.; Yasuma, T.; Momose, Y. Discovery of TAK-875: a potent, selective, and orally bioavailable GPR40 agonist. *ACS Med. Chem. Lett.* **2010**, *1*, 290–294.

(22) Christiansen, E.; Due-Hansen, M. E.; Urban, C.; Merten, N.; Pfleiderer, M.; Karlsen, K. K.; Rasmussen, S. S.; Steensgaard, M.; Hamacher, A.; Schmidt, J.; Drewke, C.; Petersen, R. K.; Kristiansen, K.; Ullrich, S.; Kostenis, E.; Kassack, M. U.; Ulven, T. Structure—Activity study of dihydrocinnamic acids and discovery of the potent FFA1 (GPR40) agonist TUG-469. *ACS Med. Chem. Lett.* **2010**, *1*, 345–349.

(23) Morrison, H.; Jona, J.; Walker, S. D.; Woo, J. C. S.; Li, L.; Fang, J. Development of a suitable salt form for a GPR40 receptor agonist. *Org. Process Res. Dev.* **2011**, *15*, 104–111.

(24) Lipinski, C. A.; Lombardo, F.; Dominy, B. W.; Feeney, P. J. Experimental and computational approaches to estimate solubility and permeability in drug discovery and development settings. *Adv. Drug Delivery Rev.* **1997**, *23*, 3–25.

(25) Gleeson, M. P. Generation of a set of simple, interpretable ADMET rules of thumb. *J. Med. Chem.* **2008**, *51*, 817–834.

(26) Hann, M. M. Molecular obesity, potency and other addictions in drug discovery. *MedChemComm* **2011**, *2*, 349–355.

(27) Hopkins, A. L.; Groom, C. R.; Alex, A. Ligand efficiency: a useful metric for lead selection. *Drug Discovery Today* **2004**, *9*, 430–431.

(28) Leeson, P. D.; Springthorpe, B. The influence of drug-like concepts on decision-making in medicinal chemistry. *Nat. Rev. Drug Discovery* **2007**, *6*, 881–890.

(29) Waring, M. J. Lipophilicity in drug discovery. *Expert Opin. Drug Discovery* **2010**, *5*, 235–248.

(30) Christiansen, E.; Due-Hansen, M. E.; Ulven, T. A rapid and efficient sonogashira protocol and improved synthesis of free fatty acid 1 (FFA1) receptor agonists. *J. Org. Chem.* **2010**, *75*, 1301–1304.

(31) Torborg, C.; Zapf, A.; Beller, M. Palladium catalysts for highly selective Sonogashira reactions of aryl and heteroaryl bromides. *ChemSusChem* **2008**, *1*, 91–96.

(32) Deng, X. H.; Mani, N. S. An efficient route to 4-aryl-5-pyrimidinylimidazoles via sequential functionalization of 2,4-dichloropyrimidine. *Org. Lett.* **2006**, *8*, 269–272.

(33) Rocca, P.; Cochennec, C.; Marsais, F.; Thomas-dit-Dumont, L.; Mallet, M.; Godard, A.; Queguiner, G. First metalation of aryl iodides: directed ortho-lithiation of iodopyridines, halogen-dance, and application to synthesis. *J. Org. Chem.* **1993**, *58*, 7832–7838.

(34) Saitton, S.; Kihlberg, J.; Luthman, K. A synthetic approach to 2,3,4-substituted pyridines useful as scaffolds for tripeptidomimetics. *Tetrahedron* **2004**, *60*, 6113–6120.

(35) Tetko, I. V.; Poda, G. I.; Ostermann, C.; Mannhold, R. Accurate in silico log P predictions: One can't embrace the unembraceable. *QSAR Comb. Sci.* **2009**, *28*, 845–849.

(36) Schmidt, J.; Smith, N. J.; Christiansen, E.; Tikhonova, I. G.; Grundmann, M.; Hudson, B. D.; Ward, R. J.; Drewke, C.; Milligan, G.; Kostenis, E.; Ulven, T. Selective orthosteric free fatty acid receptor 2 (FFA2) agonists. Identification of the structural and chemical requirements for selective activations of FFA2 versus FFA3. *J. Biol. Chem.* **2011**, *286*, 10628–10640.

(37) Pontier, C.; Pachot, J.; Botham, R.; Lenfant, B.; Arnaud, P. HT29-MTX and Caco-2/TC7 monolayers as predictive models for human intestinal absorption: role of the mucus layer. *J. Pharm. Sci.* **2001**, *90*, 1608–1619.

(38) Schroder, R.; Janssen, N.; Schmidt, J.; Kebig, A.; Merten, N.; Hennen, S.; Muller, A.; Blattermann, S.; Mohr-Andra, M.; Zahn, S.; Wenzel, J.; Smith, N. J.; Gomeza, J.; Drewke, C.; Milligan, G.; Mohr, K.; Kostenis, E. Deconvolution of complex G protein-coupled receptor signaling in live cells using dynamic mass redistribution measurements. *Nat. Biotechnol.* **2010**, *28*, 943–950.

(39) Cherezov, V.; Rosenbaum, D. M.; Hanson, M. A.; Rasmussen, S. G. F.; Thian, F. S.; Kobilka, T. S.; Choi, H. J.; Kuhn, P.; Weis, W. I.; Kobilka, B. K.; Stevens, R. C. High-resolution crystal structure of an engineered human beta(2)-adrenergic G protein-coupled receptor. *Science* **2007**, *318*, 1258–1265.

(40) Wu, B.; Chien, E. Y.; Mol, C. D.; Fenalti, G.; Liu, W.; Katritch, V.; Abagyan, R.; Brooun, A.; Wells, P.; Bi, F. C.; Hamel, D. J.; Kuhn, P.; Handel, T. M.; Cherezov, V.; Stevens, R. C. Structures of the CXCR4 chemokine GPCR with small-molecule and cyclic peptide antagonists. *Science* **2010**, *330*, 1066–1071.

(41) Rosenkilde, M. M.; Benned-Jensen, T.; Frimurer, T. M.; Schwartz, T. W. The minor binding pocket: a major player in 7TM receptor activation. *Trends Pharmacol. Sci.* **2010**, *31*, 567–574.

(42) Ballesteros, J. A.; Weinstein, H. W. In *Methods in Neuroscience*; Sealfon, S. C., Conn, P. M., Eds.; Academic Press: San Diego, CA, 1995; Vol. 25, pp 366–428.

(43) Mallet, M.; Branger, G.; Marsais, F.; Queguiner, G. Lithium migration in the pyridine series—Double catalysis and reforming—Synthesis of derivatives of 2-bromo-3-lithio-pyridine and 4-bromo-2-halogeno-3-lithio-pyridines. *J. Organomet. Chem.* **1990**, *382*, 319–332.

(44) Ullrich, S.; Berchtold, S.; Ranta, F.; Seebohm, G.; Henke, G.; Lupescu, A.; Mack, A. F.; Chao, C. M.; Su, J. P.; Nitschke, R.; Alexander, D.; Friedrich, B.; Wulff, P.; Kuhl, D.; Lang, F. Serum- and glucocorticoid-inducible kinase 1 (SGK1) mediates glucocorticoid-induced inhibition of insulin secretion. *Diabetes* **2005**, *54*, 1090–1099.

(45) Hagesaether, E. Permeation modulating properties of natural polymers. Effect of molecular weight and mucus. *Int. J. Pharm.* **2011**, *409*, 150–155.

(46) Sali, A.; Blundell, T. L. Comparative protein modeling by satisfaction of spatial restraints. *J. Mol. Biol.* **1993**, *234*, 779–815.

(47) Sum, C. S.; Tikhonova, I. G.; Costanzi, S.; Gershengorn, M. C. Two arginine—glutamate ionic locks near the extracellular surface of FFAR1 gate receptor activation. *J. Biol. Chem.* **2009**, *284*, 3529–3536.

(48) Frisch, M. J.; Trucks, G. W.; Schlegel, H. B.; Scuseria, G. E.; Robb, M. A.; Cheeseman, J. R.; Montgomery, J. A., Jr.; Vreven, T.; Kudin, K. N.; Burant, J. C.; Millam, J. M.; Iyengar, S. S.; Tomasi, J.; Barone, V.; Mennucci, B.; Cossi, M.; Scalmani, G.; Rega, N.; Petersson, G. A.; Nakatsuji, H.; Hada, M.; Ehara, M.; Toyota, K.; Fukuda, R.; Hasegawa, J.; Ishida, M.; Nakajima, T.; Honda, Y.; Kitao, O.; Nakai, H.; Klene, M.; Li, X.; Knox, J. E.; Hratchian, H. P.; Cross, J. B.; Bakken, V.; Adamo, C.; Jaramillo, J.; Gomperts, R.; Stratmann, R. E.; Yazyev, O.; Austin, A. J.; Cammi, R.; Pomelli, C.; Ochterski, J. W.; Ayala, P. Y.; Morokuma, K.; Voth, G. A.; Salvador, P.; Dannenberg, J. J.; Zakrzewski, V. G.; Dapprich, S.; Daniels, A. D.; Strain, M. C.; Farkas, O.; Malick, D. K.; Rabuck, A. D.; Raghavachari, K.; Foresman, J. B.; Ortiz, J. V.; Cui, Q.; Baboul, A. G.; Clifford, S.; Cioslowski, J.; Stefanov, B. B.; Liu, G.; Liashenko, A.; Piskorz, P.; Komaromi, I.; Martin, R. L.; Fox, D. J.; Keith, T.; Laham, A.; Peng, C. Y.; Nanayakkara, A.; Challacombe, M.; Gill, P. M. W.; Johnson, B.; Chen, W.; Wong, M. W.; Gonzalez, C.; Pople, J. A. *Gaussian 03*; Gaussian, Inc.: Wallingford, CT, 2004.

(49) Sum, C. S.; Tikhonova, I. G.; Neumann, S.; Engel, S.; Raaka, B. M.; Costanzi, S.; Gershengorn, M. C. Identification of residues important for agonist recognition and activation in GPR40. *J. Biol. Chem.* **2007**, *282*, 29248–29255.

(50) *The PyMOL Molecular Graphics System*, version 1.3; Schrodinger, LLC: New York.

(51) Case, D. A.; Darden, T. A.; Cheatham, T. E., III; Simmerling, C. L.; Wang, J.; Duke, R. E.; Luo, R.; Merz, K. M.; Pearlman, D. A.; Crowley, M.; Walker, R. C.; Zhang, W.; Wang, B.; Hayik, S.; Roitberg, A.; Seabra, G.; Wong, K. F.; Paesani, F.; Wu, X.; Brozell, S.; Tsui, V.; Gohlke, H.; Yang, L.; Tan, C.; Mongan, J.; Hornak, V.; Cui, G.; Beroza, P.; Mathews, D. H.; Schafmeister, C.; Ross, W. S.; Kollman, P. A. *AMBER 9*; University of California, San Francisco: San Francisco, CA, 2006.

(52) Duan, Y.; Wu, C.; Chowdhury, S.; Lee, M. C.; Xiong, G. M.; Zhang, W.; Yang, R.; Cieplak, P.; Luo, R.; Lee, T.; Caldwell, J.; Wang, J. M.; Kollman, P. A point-charge force field for molecular mechanics simulations of proteins based on condensed-phase quantum mechanical calculations. *J. Comput. Chem.* **2003**, *24*, 1999–2012.